

CONFIDENTIAL

Copy 13  
RM SL56L24

NACA



# RESEARCH MEMORANDUM

for the

U. S. Air Force

STATIC STABILITY AND CONTROL CHARACTERISTICS OF A

0.04956-SCALE MODEL OF THE CONVAIR F-102A

AIRPLANE AT TRANSONIC SPEEDS

By Walter B. Olstad and Robert S. Osborne

Langley Aeronautical Laboratory  
Langley Field, Va.

**LIBRARY COPY**

JAN 4 1957

LANGLEY AERONAUTICAL LABORATORY  
LIBRARY NACA  
LANGLEY FIELD, VIRGINIA

CLASSIFIED DOCUMENT

This material contains information affecting the National Defense of the United States within the meaning of the espionage laws, Title 18, U.S.C., Secs. 793 and 794, the transmission or revelation of which in any manner to an unauthorized person is prohibited by law.

**NATIONAL ADVISORY COMMITTEE  
FOR AERONAUTICS  
WASHINGTON**

CONFIDENTIAL

Convair MX-1554  
(YF-102)

NACA RM SL56L24

NATIONAL ADVISORY COMMITTEE FOR AERONAUTICS

RESEARCH MEMORANDUM

for the

U. S. Air Force

STATIC STABILITY AND CONTROL CHARACTERISTICS OF A

0.04956-SCALE MODEL OF THE CONVAIR F-102A

AIRPLANE AT TRANSONIC SPEEDS

By Walter B. Olstad and Robert S. Osborne

SUMMARY

The effects of elevator deflections from  $0^\circ$  to  $-10^\circ$  on the force and moment characteristics of a 0.04956-scale model of the Convair F-102A airplane have been determined at Mach numbers from 0.60 to 1.135 for angles of attack up to  $20^\circ$  in the Langley 8-foot transonic tunnel. The model was tested with a plane wing to indicate the effects of wing leading-edge camber and deflected tips. In addition, the basic model was tested at angles of sideslip from  $-10^\circ$  to  $4^\circ$  at an angle of attack of  $2.2^\circ$ .

The results indicated that the configuration was longitudinally stable for all conditions tested; however, a possible mild pitch-up tendency was indicated for a lift coefficient of about 0.6 at a Mach number of 0.60. Elevator pitch and lift effectiveness decreased rapidly at Mach numbers above 0.90, but no complete loss or reversal was indicated for lift coefficients up to at least 0.7. Wing and body modifications have resulted in an increase in maximum trimmed lift-drag ratio of slightly more than 1.0 for the F-102A over that for the original F-102, and the drag for trimmed level flight has been substantially reduced for medium and high altitudes. At the low angle of attack tested, the configuration had approximately neutral effective dihedral and positive directional stability through the Mach number range.

INTRODUCTION

At the request of the U. S. Air Force, approximately 1/20-scale models of various configurations of the Convair F-102 airplane have been tested at transonic speeds in the Langley 8-foot transonic tunnel to determine their stability, control, and performance characteristics.

Previous investigations of the original F-102 configuration (refs. 1 and 2) indicated that the wave drag, drag due to lift, and trim drag should be appreciably reduced in order to improve its medium- and high-altitude performance. In order to reduce the wave drag, the fuselage was lengthened and indented as prescribed by the supersonic area rule to give a smooth total area distribution at a design Mach number of 1.2 (refs. 3 and 4). The drag due to lift was improved by cambering the wing leading edge (ref. 5), and the trim drag was decreased by deflecting the trailing edge of the wing tips upward  $10^\circ$  about the elevator hinge line extended (ref. 5). Upon assemblage of these various modifications into the F-102A configuration, it was found that the original fence configuration was no longer suitable for alleviating the moderate-lift pitch-up tendency (ref. 6), and a new arrangement of chordwise fences was determined from the results of reference 7.

A 0.04956-scale model of this later F-102A configuration was then tested to determine the effects of elevator deflections from  $0^\circ$  to  $-10^\circ$  on the force and moment characteristics for Mach numbers from 0.6 to 1.135 and angles of attack up to  $20^\circ$ . Tests were also made through the same Mach number range for angles of sideslip from  $-10^\circ$  to  $4^\circ$  at an angle of attack of  $2.2^\circ$ . In addition, in order to indicate the effects of wing leading-edge camber and deflected tips, the model was tested with a plane  $60^\circ$  delta wing at angles of attack up to  $12^\circ$ . The results are presented herein.

#### SYMBOLS

b	wing span, in.
$C_D$	drag coefficient, $D/qS$
$C_{D,0}$	drag coefficient at zero lift
$\frac{\partial C_D}{\partial C_L^2}$	drag-due-to-lift factor, averaged from $C_L = 0$ to $C_L = 0.3$
$C_L$	lift coefficient, $L/qS$
$C_{L,(L/D)_{\max}}$	lift coefficient for maximum lift-drag ratio
$C_{L\alpha}$	lift-curve slope per degree, averaged from $\alpha = 0^\circ$ over linear portion of curve

$C_{L\delta}$	lift effectiveness parameter at constant angle of attack
$C_l$	rolling-moment coefficient, $M_{X_S}/qSb$
$C_{l\beta}$	effective dihedral parameter, $\frac{\partial C_l}{\partial \beta}$ , per deg
$C_m$	pitching-moment coefficient, $M_Y/qS\bar{c}$
$\frac{\partial C_m}{\partial C_L}$	static longitudinal stability parameter
$\frac{\partial C_m}{\partial \delta}$	pitch-effectiveness parameter averaged at constant lift coefficient
$C_n$	yawing-moment coefficient, $M_{Z_S}/qSb$
$C_{n\beta}$	static directional stability parameter, $\frac{\partial C_n}{\partial \beta}$ , per deg
$C_Y$	lateral-force coefficient, $Y/qS$
$C_{Y\beta}$	lateral-force derivative, $\frac{\partial C_Y}{\partial \beta}$ , per deg
$\bar{c}$	wing mean aerodynamic chord, in.
$D$	drag, lb
$L$	lift, lb
$(L/D)_{\max}$	maximum lift-drag ratio
$M$	free-stream Mach number
$M_{X_S}$	moment about $X_S$ -axis, in-lb (see fig. 2)
$M_Y$	moment about $Y$ -axis, in-lb (see fig. 2)
$M_{Z_S}$	moment about $Z_S$ -axis, in-lb (see fig. 2)

q	free-stream dynamic pressure, lb/sq ft
R	Reynolds number
S	total wing area, sq ft
Y	lateral force, lb
$\alpha$	angle of attack of wing chord line with no leading-edge camber, deg
$\beta$	angle of sideslip, deg
$\delta$	elevator deflection measured at right angles to hinge line and positive when trailing edge is down, deg

## APPARATUS AND TESTS

### Tunnel

The tests were conducted in the Langley 8-foot transonic tunnel, which is a dodecagonal, slotted-throat, single-return tunnel designed to obtain aerodynamic data through the speed of sound while minimizing the usual effects of choking and blockage. The tunnel operates at approximately atmospheric stagnation pressures. A description of test-section design and flow uniformity is available in references 8 and 9.

### Model

The 0.04956-scale model of the Convair F-102A airplane used in this investigation was supplied by the contractor. Dimensional details of the model are presented in figure 1 and table I.

The basic F-102A wing was derived from a plane  $60^\circ$  delta wing with modified NACA 0004-65 streamwise airfoil sections (see ref. 1) by extending the leading edge approximately 4.1 percent of the mean aerodynamic chord, which increased the leading-edge sweep angle to  $60.14^\circ$ , and conically cambering the outboard 6.37 percent of the local semispan for a design lift coefficient of 0.15 at a Mach number of approximately 1.0 (see ref. 5). The trailing edges of the wing tips outboard of the 82-percent-semispan station were deflected upward  $10^\circ$  about the elevator hinge line extended. The wing was constructed with a steel core covered by a tin-bismuth surface. Aluminum-alloy leading edges and steel tips were removable, which allowed the F-102A model to be tested with plane uncambered leading edges and undeflected tips (hereinafter referred to as the plane wing).

Installed on the basic (cambered) wing were two sets of chordwise fences. Upper-surface fences extending from 1.8 to 33 percent of the local chord were located at the 35-percent-semispan station, and wrap-around fences extending from 22.7 percent of the local chord on the lower surface around the leading edge to 67 percent of the chord on the upper surface were located at the 66-percent-semispan station. On the plane wing and located at the 66-percent-semispan station were chordwise fences extending from the leading edge along the upper surface to 80 percent of the local chord.

The fuselage was equipped with ram inlets which were closed for these tests by means of faired plugs (see fig. 1). The fuselage was designed using the supersonic area-rule concept and was indented for the wing and tail in order to give a favorable total area distribution at a design Mach number of 1.2. Additional details of the wing and fuselage including cross-sectional area distributions are presented in reference 6.

The vertical tail had a  $60^\circ$  sweptback leading edge, a  $5^\circ$  sweptforward trailing edge, and used NACA 0004-65 (mod.) streamwise airfoil sections. A flat-plate antenna was located just above the rudder.

The configuration had no horizontal tail. The elevators were wing trailing-edge flaps deflected about hinge lines perpendicular to the model center line. The gap ahead of the hinge line was sealed. The total elevator area rearward of the hinge line was 9.7 percent of the total wing area.

#### Model Support System

The model was attached to a sting support through an electrical six-component strain-gage balance located inside the fuselage. The sting support was cylindrical for 2.8 base diameters downstream of the model base and was fixed on the tunnel axis by two sets of struts projecting from the tunnel walls. Angled couplings in the sting were employed to maintain the model position near the tunnel center line at all angles of attack.

#### Measurements and Accuracy

Model forces and moments were measured by a six-component internal strain-gage balance and converted to lift, drag, pitching moment, lateral force, yawing moment, and rolling moment about stability axes (see fig. 2) originating at a center-of-gravity location at 29.6 percent of the wing mean aerodynamic chord (27.5 percent for the plane wing) and 4.5 percent of the mean aerodynamic chord above the wing chord plane. Accuracies of the coefficients are estimated to be within the following limits:

$C_L$	$\pm 0.005$ through $C_L$ range
$C_D$	$\pm 0.001$ through $C_L \approx 0.4$
$C_m$	$\pm 0.001$ through $C_L$ range
$C_{L_z}$	$\pm 0.0002$ through $C_L$ range
$C_{n_z}$	$\pm 0.0003$ through $C_L$ range
$C_Y$	$\pm 0.002$ through $C_L$ range

The angles of attack and sideslip were determined to within  $\pm 0.15^\circ$  by a pendulum-type inclinometer located in the sting support and from a calibration of sting and balance deflection with respect to model load. Elevator control deflections are estimated to be accurate within  $\pm 0.2^\circ$ .

The Mach number was determined to within 0.003 from a calibration with respect to test chamber pressure. Base pressures used to adjust the drag data were obtained from an orifice located inside the model 2 inches forward of the plane of the base. Base pressure coefficients for the configuration with controls undeflected are available in reference 7.

#### Tests

The basic model was tested at Mach numbers from 0.6 to 1.135 at angles of attack from  $0^\circ$  to approximately  $20^\circ$  with elevator deflections of  $0^\circ$ ,  $-2.5^\circ$ ,  $-5.0^\circ$ ,  $-7.5^\circ$ , and  $-10.0^\circ$ . At the higher Mach numbers, the maximum attainable angle of attack was reduced to less than  $20^\circ$  by tunnel power and balance limitations. The model with elevators undeflected was also tested through the same Mach number range at angles of sideslip from  $-10^\circ$  to  $4^\circ$  at a constant angle of attack of  $2.2^\circ$  with and without the vertical tail. The plane-wing configuration with elevators undeflected was tested through the Mach number range at angles of attack from  $0^\circ$  to about  $12^\circ$ . All tests were made with the inlets faired closed.

The average test Reynolds number based on the wing mean aerodynamic chord varied from  $4.0 \times 10^6$  to  $4.8 \times 10^6$  over the Mach number range (fig. 3).

#### Corrections

Subsonic boundary interference is minimized by the slotted test section, and no corrections for this interference have been applied. The effects of supersonic boundary-reflected disturbances were reduced by testing the model several inches from the tunnel center line. However, it is possible that these disturbances caused small errors in the drag and pitching-moment measurements at Mach numbers of 1.075 and 1.135. It

is believed, however, that these errors would have little effect upon the majority of the faired data plotted against Mach number in the summary and analysis plots and that indicated trends are independent of boundary-reflected disturbances.

No corrections for sting interference have been applied. The drag data have been adjusted to an assumed condition of free-stream static pressure acting over the model base.

## RESULTS

All data presented herein are for a condition with the air inlets faired closed. However, a comparison between the present data for the basic configuration with controls undeflected and unpublished data obtained on the same model with a slightly different fence arrangement but with the inlets open and operating at inlet mass-flow ratios from 0.75 to 0.85 indicated drag coefficient agreement within approximately 0.001 over the lift and Mach number range tested.

The longitudinal characteristics of the basic model with various elevator deflections are presented as a function of lift coefficient at constant Mach number in figure 4. The lift coefficients required for level flight of the F-102A airplane at a combat wing loading of 36 lb/sq ft for altitudes from sea level to 60,000 feet are presented in figure 5. These flight conditions are the basis for a summary and brief analysis of the longitudinal characteristics presented in figures 6 to 12.

A comparison of the trimmed drag characteristics for the present F-102A configuration with those for the original F-102 model as reported in reference 2 is shown in figures 13 and 14. Because of model scale deviations, a small drag correction has been applied to the data of reference 2. Details of this correction are available in reference 5.

The longitudinal characteristics of the plane-wing and the basic or cambered-wing configurations are compared as a function of lift coefficient in figure 15. The coefficients are based on the actual wing area of each configuration.

The variation of rolling-moment, yawing-moment, lateral-force, lift, drag, and pitching-moment coefficients with angle of sideslip at constant Mach number for an angle of attack of  $2.2^\circ$  is presented in figures 16 to 19 for the basic configuration with and without the vertical tail. Lateral-directional stability characteristics are summarized as a function of Mach number in figure 20. The values were obtained by taking an average slope over the linear portions of the curves through  $\beta = 0^\circ$ .

## DISCUSSION

## Longitudinal Characteristics

Static longitudinal stability.- The basic F-102A configuration exhibited static longitudinal stability for all elevator deflections tested throughout the investigated lift coefficient and Mach number range (fig. 4). The decrease in static margin to near neutral stability at a trim lift coefficient of about 0.6 at a Mach number of 0.60 (fig. 4(a)) indicated the possibility of mild pitch-up in this region; however, the tendency was not apparent at Mach numbers of 0.85 and above, and it generally appeared that the chordwise fences installed on the wing had been effective in alleviating the severe moderate-lift pitch-up tendency indicated for the configuration without fences in reference 7. The rapid decrease in pitching moment beginning at a lift coefficient of approximately 0.7 for the larger elevator deflection cases at Mach numbers of 0.85 and 0.90 (figs. 4(b) and 4(c)) can be associated with the wing stall indicated by the lift curves to have occurred at an angle of attack of about  $20^\circ$ .

The values of the static longitudinal stability parameter  $\partial C_m / \partial C_L$  taken at lift coefficients for trimmed level flight for altitudes from 20,000 feet to 60,000 feet varied from about -0.06 at a Mach number of 0.60 to approximately -0.18 at Mach numbers above 1.0 (fig. 6), indicating a rearward shift in aerodynamic-center location of about 12 percent of the mean aerodynamic chord. It should be noted that this shift in the aerodynamic-center location was rather irregular for Mach numbers from 0.90 to 1.025 and caution should be exercised in this region. The effects of increasing altitude on the parameter were generally small.

Elevator pitch effectiveness.- Positive elevator effectiveness was indicated through the Mach number range tested for lift coefficients up to at least 0.7 (fig. 4). In this range, elevator effectiveness at a given Mach number was generally constant for the deflection angles tested, except that at Mach numbers from about 0.85 to 0.95 some decrease was indicated with a change in control deflection from  $-7.5^\circ$  to  $-10^\circ$ . The average value of the elevator pitch effectiveness parameter  $\partial C_m / \partial \delta$  taken at constant lift coefficients from 0 to 0.5 at  $C_m = 0$  reached a maximum of -0.0084 at a Mach number of 0.925 and then decreased rapidly to -0.0034 at a Mach number of 1.135 - a decrease of approximately 60 percent (see fig. 6).

Trim elevator settings.- Elevator deflections required for trimmed level flight at several altitudes for a wing loading of 36 lb/sq ft are presented in figure 7. The up elevator required decreased steadily with increases in Mach number from 0.6 to 0.925. Rapid increases in up elevator, an indication of control-position instability, were required at

altitude at Mach numbers above 0.925. These effects were magnified with increasing altitude, as would be expected. The data for the Mach numbers of 1.075 and 1.135 may have been affected somewhat by the presence of boundary-reflected disturbances on the rear of the model.

Lift-curve slopes.- The lift curves for the various elevator angles at constant Mach number were generally linear for angles of attack up to  $12^\circ$  or  $16^\circ$  (fig. 4). The lift-curve slope averaged over the linear portion of the curve varied from 0.046 to 0.058 for the  $0^\circ$  elevator case (fig. 8). With increases in elevator deflection, minor increases in average lift-curve slope were indicated at Mach numbers above 0.95 (fig. 4).

Trimming the configuration reduced the untrimmed ( $\delta = 0^\circ$ ) lift-curve slope by 15 to 25 percent. This large loss is a result of the type of longitudinal control used. The trailing-edge flap type of elevators have a relatively short effective tail length and, therefore, require large areas and deflections in order to produce the necessary longitudinal balancing moments. Consequently, when the elevators are deflected trailing edge up, the lift at a given angle of attack is substantially reduced. This loss in lift due to trimming the configuration is not quite so severe for the current model as it was for the F-102 (ref. 2) because of the deflected wing tips which reduces the out-of-trim pitching moment.

Elevator lift effectiveness.- The elevator lift effectiveness parameter  $C_{L\delta}$  at constant angle of attack decreased from 0.019 at a Mach number of 0.9 to 0.0125 for Mach numbers above 0.975 (fig. 8). These values are applicable to and have been averaged over an angle-of-attack range from  $0^\circ$  to  $8^\circ$  for elevator deflections from  $0^\circ$  to  $-10^\circ$ .

Drag characteristics.- The zero-lift transonic drag rise for the configuration with controls undeflected began at a Mach number of about 0.91 (fig. 9). The magnitude of the drag rise was approximately 0.015 between the Mach numbers of 0.90 and 1.075.

For the zero elevator condition the drag-due-to-lift factor  $\partial C_D / \partial C_L^2$ , averaged over a lift-coefficient range from 0 to 0.3, remained essentially constant at 0.24 over the Mach number range tested (fig. 9). This represents an approximate 7-percent decrease in drag-due-to-lift factor for the F-102A model as compared with that of the F-102 (ref. 2). A comparison of the drag-due-to-lift factor for the F-102A with theoretical computations for full leading-edge suction and no leading-edge suction indicated that approximately 55 percent full leading-edge suction was being realized.

A comparison of the lift-drag polars for the zero-elevator deflection case with those for trimmed conditions (fig. 10) indicated a sizeable penalty in drag at lift coefficients above 0.2 due to trimming the configuration. However, a comparison of the increment due to trimming

of the drag-due-to-lift factor for the F-102A (fig. 9) and the F-102 (ref. 2) indicated a reduction in this increment for the F-102A of the order of 60 to 70 percent throughout the Mach number range. This saving in trim drag is largely a result of the deflected wing tips on the F-102A which effectively increased the elevator area and thereby reduced the elevator deflection required for trimmed level flight.

Lift-drag ratios.- The maximum lift-drag ratio for the configuration with elevators undeflected decreased from approximately 10.0 at a Mach number of 0.6 to approximately 6.0 at Mach numbers above 1.0 (fig. 11). The lift coefficient for maximum lift-drag ratio increased from approximately 0.22 at a Mach number of 0.6 to 0.32 at a Mach number of 1.075. Trimming the configuration had little effect upon the maximum lift-drag ratio at subcritical speeds, but reduced the maximum lift-drag ratio by approximately 1.0 for Mach numbers above 1.0.

A comparison of the lift-drag ratios for trimmed level flight at several altitudes with the maximum possible trimmed lift-drag ratios is presented in figure 12. This comparison illustrates the need for an increase in altitude for most efficient flight with increasing Mach number.

Drag comparison with F-102.- The drag values for trimmed level flight at several altitudes have been broken down into several components in order to show their relative importance for various flight conditions (fig. 13). The first component, zero-lift drag, has been taken as the drag at zero-lift coefficient for the configuration with elevators undeflected and consists of the skin-friction drag and the minimum wave drag. The drag-due-to-lift component is the difference between the zero-lift drag and the drag at the lift coefficient required with the elevators undeflected. This component is a function of wing characteristics such as aspect ratio and camber. The leading edge of the basic F-102A wing has been cambered in order to realize a greater percentage of full leading-edge suction and thereby reduce this drag-due-to-lift component of drag. The final component, trim drag, is that increment in drag caused by trimming the configuration from the zero elevator condition. It depends upon the type of control, control effectiveness, and magnitude of the out-of-trim pitching moments.

A comparison of the total drag at trimmed level flight for the F-102A and the F-102 of reference 2 is also presented in figure 13. This shows a reduction in the drag of the F-102A from that of the F-102 amounting to approximately 11 to 24 percent over the Mach number range of 0.85 to 1.1 at an altitude of 40,000 feet and approximately 15 to 28 percent at an altitude of 60,000 feet. This reduction in drag has been realized through a combination of modifications, namely: body indentation, wing leading-edge camber, and wing-tip deflection.

A comparison of the drag results of the F-102A with those for the F-102 indicated that the modifications to the fuselage and wings have

increased the maximum trimmed lift-drag ratio by slightly more than 1.0 throughout the Mach number range (fig. 14). The F-102A configuration shows a higher value of lift coefficient for maximum trimmed lift-drag ratio for the Mach numbers tested indicating that the F-102A is capable of its most efficient flight at higher altitudes than the F-102.

Comparison of basic- and plane-wing configuration.- Data with controls undeflected for the F-102A model with a plane wing and for the model with the basic cambered wing leading edges and deflected tips are compared in figure 15. Cambering the wing leading edge resulted in small increases in drag at low lift coefficients through the Mach number range, but substantial decreases in drag were realized at lift coefficients above about 0.15. Deflecting the wing tips had the beneficial effect of increasing the pitching moment at a given lift without changing the slope of the pitch curve, the result being a decrease in out-of-trim pitching moment at lift coefficients above approximately 0.05. These results confirm those of reference 5.

#### Lateral-Directional Characteristics

Effective dihedral.- The effective dihedral ( $-C_{l\beta}$ ) for the configuration without the vertical tail was slightly negative for an angle of attack of  $2.2^\circ$  throughout the Mach number range (figs. 16 and 20). Addition of the vertical tail contributed a small stabilizing component to the effective dihedral of the configuration, and the value of  $C_{l\beta}$  for the complete model varied from approximately zero at Mach numbers below 0.975 to  $-0.0006$  at a Mach number of 1.135. It should be noted, however, that the effective dihedral of sweptback wings generally increases with increases in angle of attack. (See, for example, ref. 10.)

Directional stability.- The variations of yawing moment with sideslip angle were generally linear through the Mach number range for the model with vertical tail on and off (fig. 17). The configuration without the vertical tail was directionally unstable (fig. 20). With the addition of the vertical tail the configuration became directionally stable and had a value of  $C_{n\beta}$  of approximately 0.0014 throughout most of the Mach number range. At high angles of attack the directional stability of the configuration would probably decrease substantially and might become negative as the vertical tail became blanketed by the rather large wing surface. This loss of vertical tail effectiveness was noted in reference 11.

The lateral-force derivatives for the configuration with and without the vertical tail were only slightly affected by changes in Mach number (figs. 18 and 20). The increment in lateral-force derivative  $C_{Y\beta}$  due to the vertical tail was approximately  $-0.007$  throughout the Mach number range.

Lift, drag, and pitching-moment coefficients.- Little effect of sideslip angle on the lift and drag coefficients was noted (fig. 19). For the complete model, the trim change appeared to be negligible throughout the sideslip angle range investigated.

### CONCLUSIONS

An investigation of static stability and control characteristics of a 0.04956-scale model of the Convair F-102A airplane at transonic speeds indicated the following conclusions:

1. The configuration exhibited static longitudinal stability for all conditions tested; however, a possible mild pitch-up tendency was indicated at a lift coefficient of 0.6 and a Mach number of 0.60.
2. A rapid decrease in elevator pitch and lift effectiveness occurred at Mach numbers above 0.90, but no complete loss or reversal was indicated for lift coefficients up to at least 0.7.
3. The application of body modifications, wing leading-edge camber, and wing-tip deflection has resulted in increasing the maximum trimmed lift-drag ratio of the F-102A over that of the F-102 by slightly more than 1.0 and has substantially reduced the drag for trimmed level flight at medium and high altitudes.
4. At the low angle of attack tested, the configuration exhibited approximately neutral effective dihedral and positive directional stability through the Mach number range.

Langley Aeronautical Laboratory,  
National Advisory Committee for Aeronautics,  
Langley Field, Va., December 4, 1956.

Approved: *Eugene C. Draley*  
Eugene C. Draley  
Chief of Full-Scale Research Division

*Walter B. Olstad*  
Walter B. Olstad  
Aeronautical Research Engineer

*Robert S. Osborne*  
Robert S. Osborne  
Aeronautical Research Engineer

DY

## REFERENCES

1. Osborne, Robert S., and Wornom, Dewey E.: Aerodynamic Characteristics Including Effects of Wing Fixes of a 1/20-Scale Model of the Convair F-102 Airplane at Transonic Speeds. NACA RM SL54C23, U. S. Air Force, 1954.
2. Osborne, Robert S., and Tempelmeyer, Kenneth E.: Longitudinal Control Characteristics of a 1/20-Scale Model of the Convair F-102 Airplane at Transonic Speeds. NACA RM SL54G15, U. S. Air Force, 1954.
3. Wornom, Dewey E., and Osborne, Robert S.: Effects of Body Indentation on the Drag Characteristics of a Delta-Wing—Body Combination at Transonic Speeds. NACA RM L54K12a, 1955.
4. Kelly, Thomas C., and Osborne, Robert S.: Effects of Fuselage Modifications on the Drag Characteristics of a 1/20-Scale Model of the Convair F-102 Airplane at Transonic Speeds. NACA RM SL54K18a, U. S. Air Force, 1954.
5. Tempelmeyer, Kenneth E., and Osborne, Robert S.: Effects of Wing Leading-Edge Camber and Tip Modifications on the Aerodynamic Characteristics of a 1/20-Scale Model of the Convair F-102 Airplane at Transonic Speeds. NACA RM SL54K29, U. S. Air Force, 1954.
6. Tempelmeyer, Kenneth E., and Osborne, Robert S.: Aerodynamic Characteristics of a 0.04956-Scale Model of the Convair F-102A Airplane at Transonic Speeds. NACA RM SL55D19, U. S. Air Force, 1955.
7. Osborne, Robert S.: Effects of Wing Modifications on the Longitudinal Stability Characteristics of a 0.04956-Scale Model of the Convair F-102A Airplane at Transonic Speeds. NACA RM SL56J30a, U. S. Air Force, 1956.
8. Wright, Ray H., and Ritchie, Virgil S.: Characteristics of a Transonic Test Section With Various Slot Shapes in the Langley 8-Foot High-Speed Tunnel. NACA RM L51H10, 1951.
9. Ritchie, Virgil S., and Pearson, Albin O.: Calibration of the Slotted Test Section of the Langley 8-Foot Transonic Tunnel and Preliminary Experimental Investigation of Boundary-Reflected Disturbances. NACA RM L51K14, 1952.
10. Polhamus, Edward C., and Sleeman, William C., Jr.: The Rolling Moment Due to Sideslip of Swept Wings at Subsonic and Transonic Speeds. NACA RM L54L01, 1955.

11. Goodman, Alex, and Thomas, David F., Jr.: Effects of Wing Position and Fuselage Size on the Low-Speed Static and Rolling Stability Characteristics of a Delta-Wing Model. NACA Rep. 1224, 1955. (Supersedes NACA TN 3063.)

TABLE I

DIMENSIONS OF A 0.04956-SCALE MODEL OF THE F-102A AIRPLANE

Basic (cambered) wing:

Airfoil section . . . . .	Modified NACA 0004-65 with leading-edge camber and wing tips outboard of $0.82b/2$ deflected upward $10^\circ$ about elevator hinge line extended	
Total area, sq ft . . . . .		1.709
Aspect ratio . . . . .		2.1
Taper ratio . . . . .		0
Incidence, deg . . . . .		0
Dihedral, deg . . . . .		0
Elevator area rearward of hinge line, sq ft . . . . .		0.166

Plane wing:

Airfoil section . . . . .	Modified NACA 0004-65	
Total area, sq ft . . . . .		1.625
Aspect ratio . . . . .		2.2
Taper ratio . . . . .		0
Incidence, deg . . . . .		0
Dihedral, deg . . . . .		0

Vertical tail:

Airfoil section . . . . .	Modified NACA 0004-65	
Exposed area, sq ft . . . . .		0.1704
Aspect ratio . . . . .		1.1
Taper ratio . . . . .		0

Fuselage:

Length, in. . . . .		34.161
Frontal area (less canopy), sq ft . . . . .		0.0826
Fineness ratio (less canopy) . . . . .		8.75
Total base area, sq ft . . . . .		0.0236

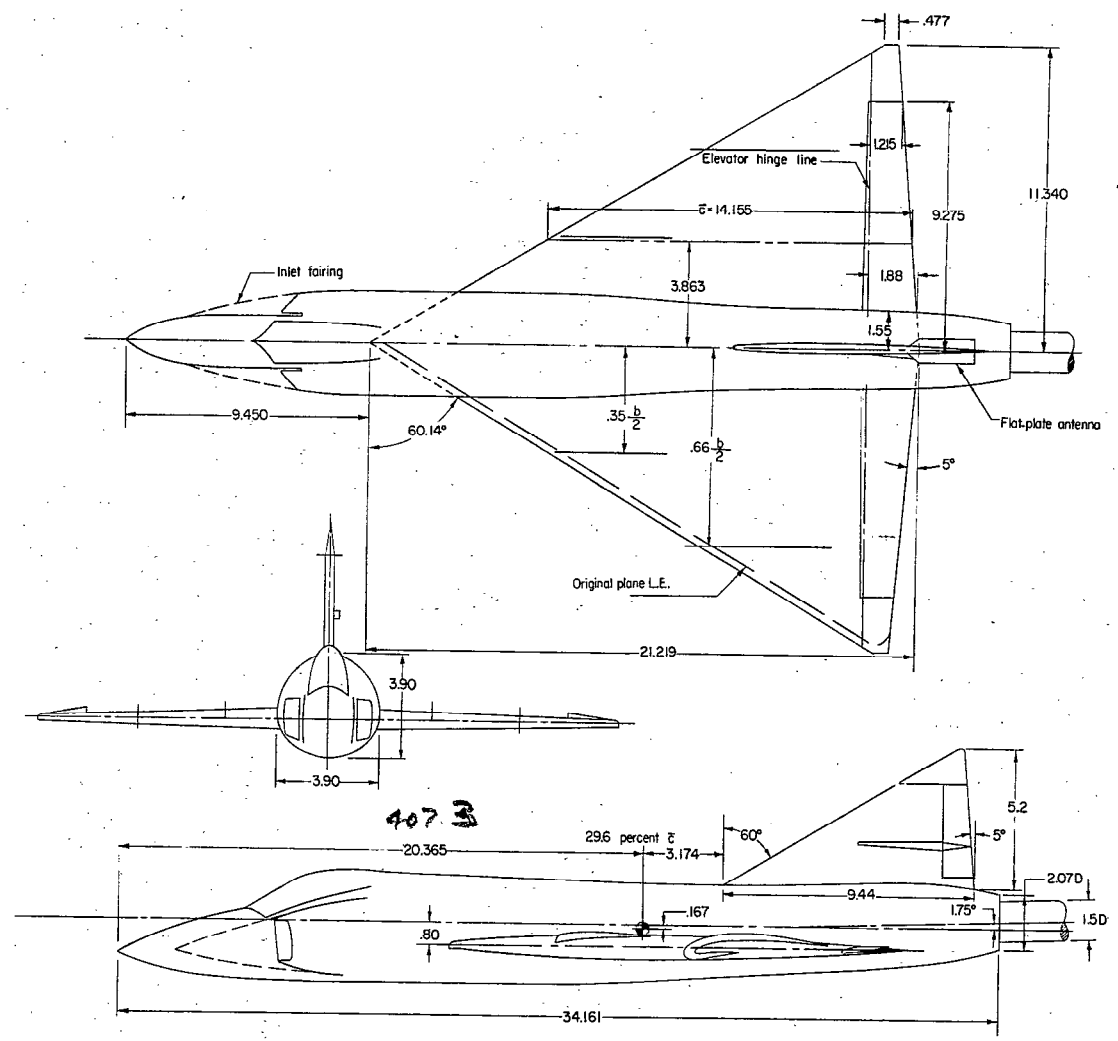


Figure 1.- Three-view drawing of a 0.04956-scale model of the Convair F-102A airplane. All dimensions in inches unless otherwise noted.

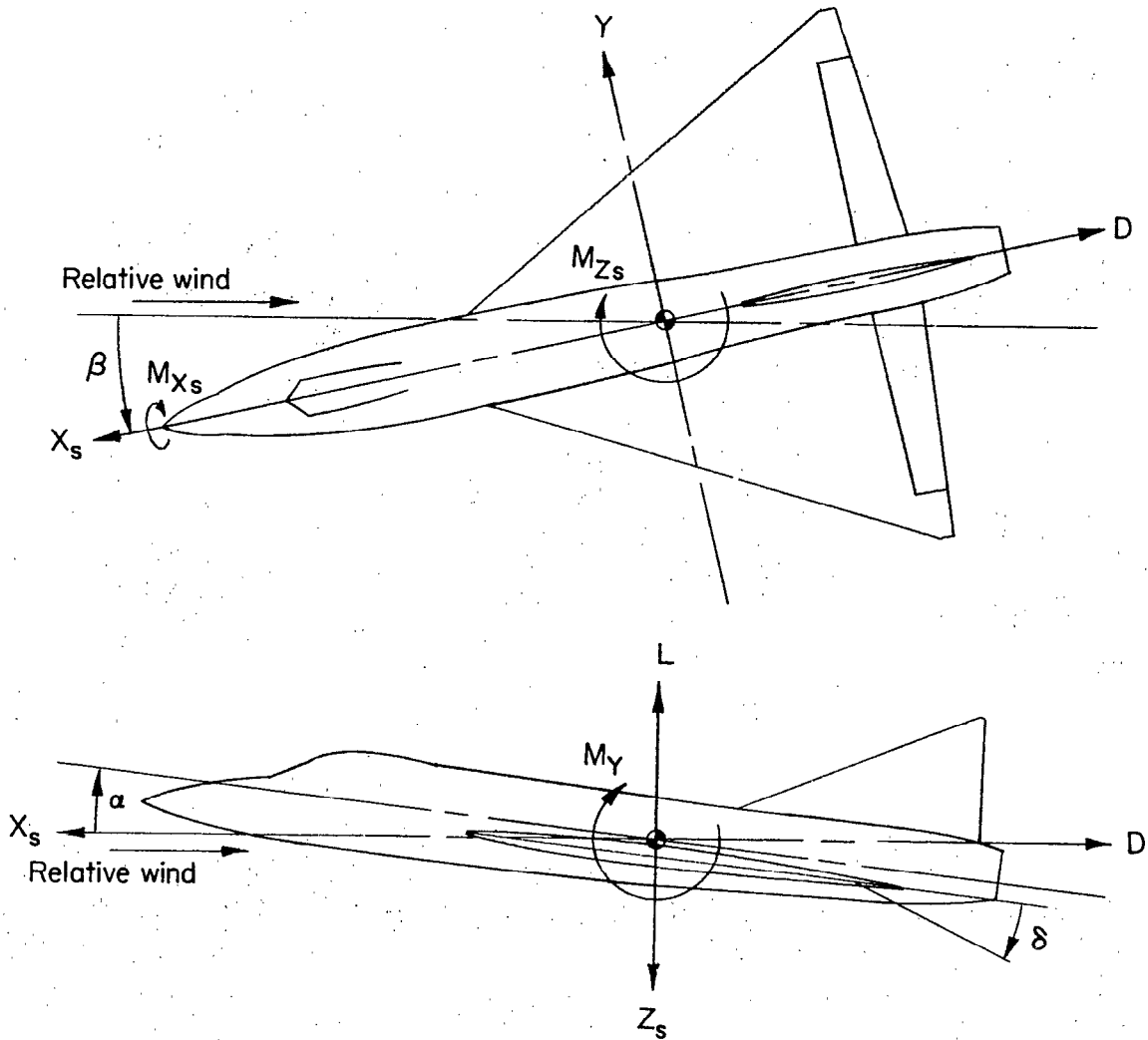


Figure 2.- System of stability axes. Arrows indicate positive directions.

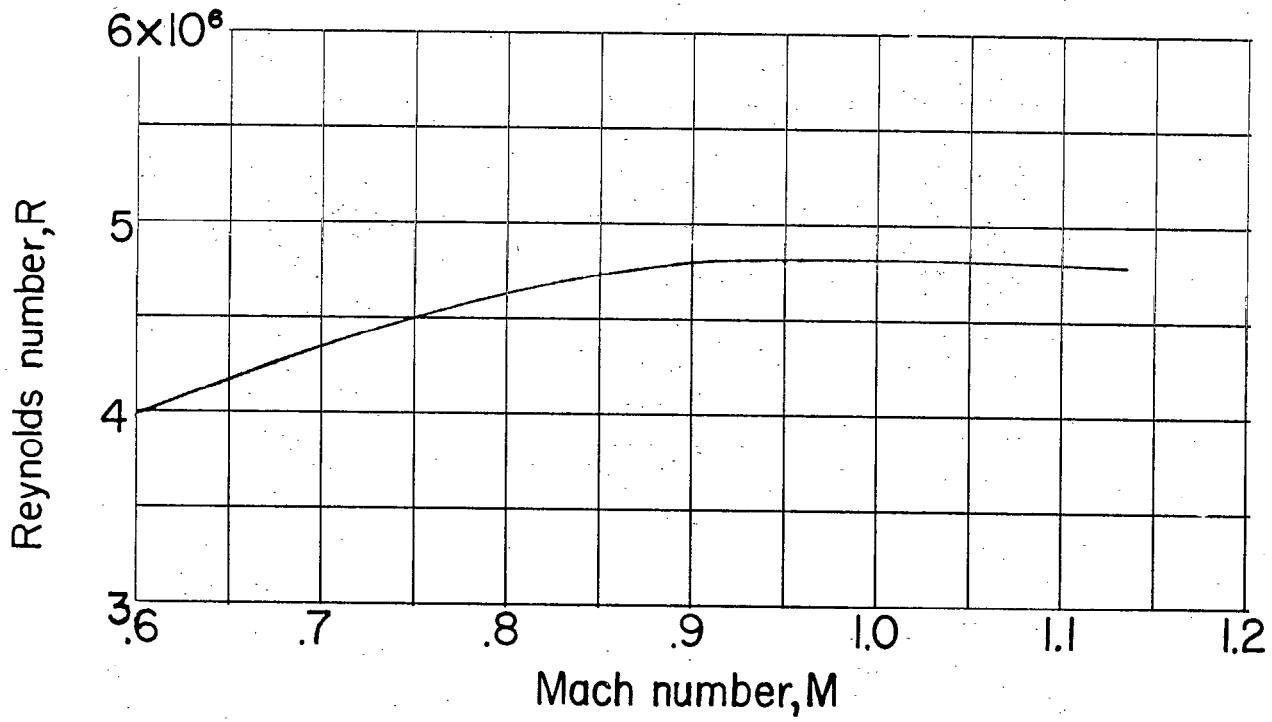
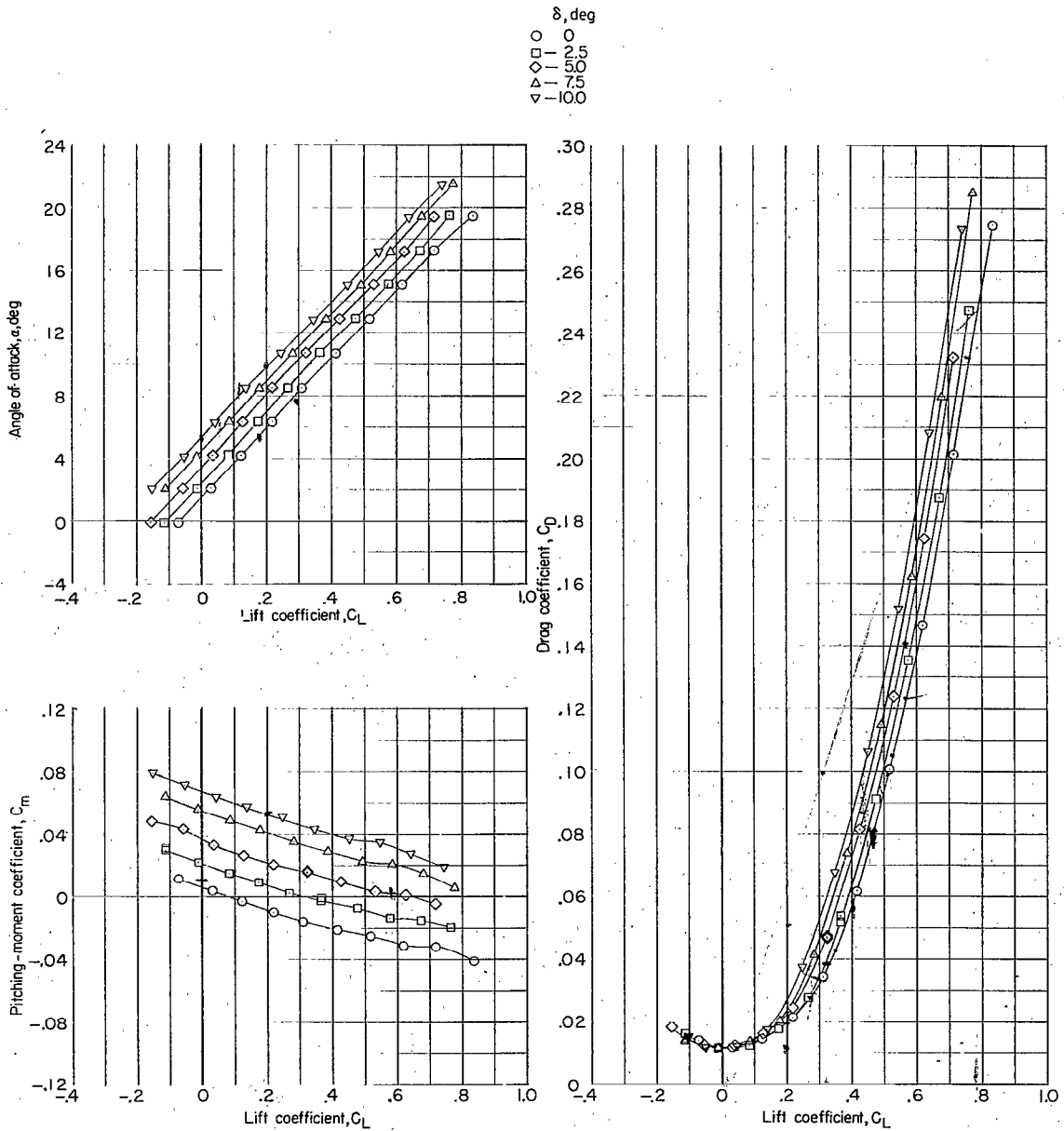


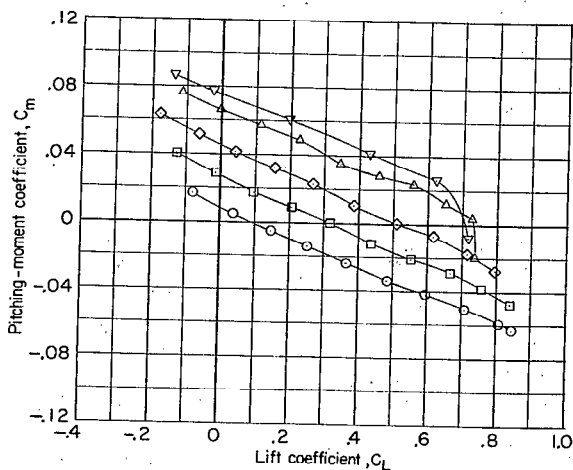
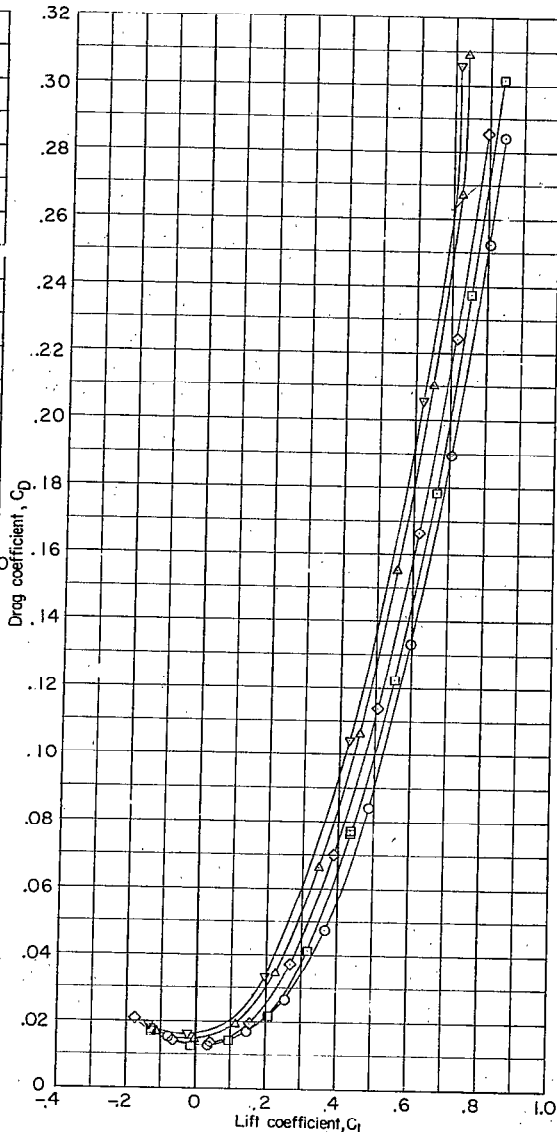
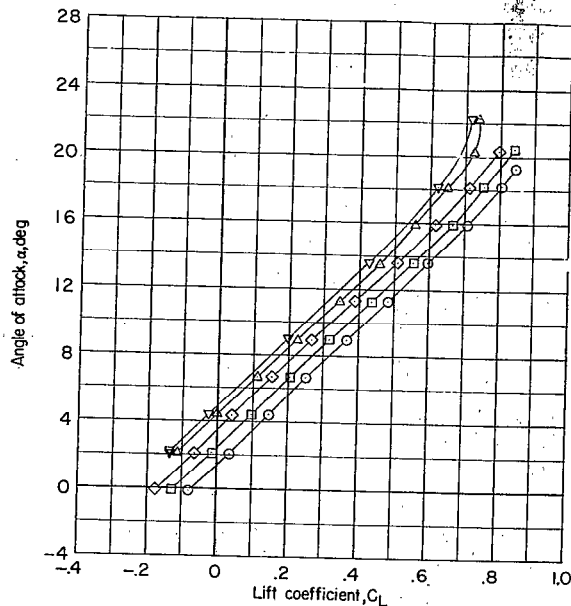
Figure 3.- Variation with Mach number of the approximate test Reynolds number based on  $\bar{c} = 14.155$  inches.



(a)  $M = 0.60$ .

Figure 4.- Longitudinal characteristics of the model with various elevator deflections.  $\beta = 0^\circ$ .

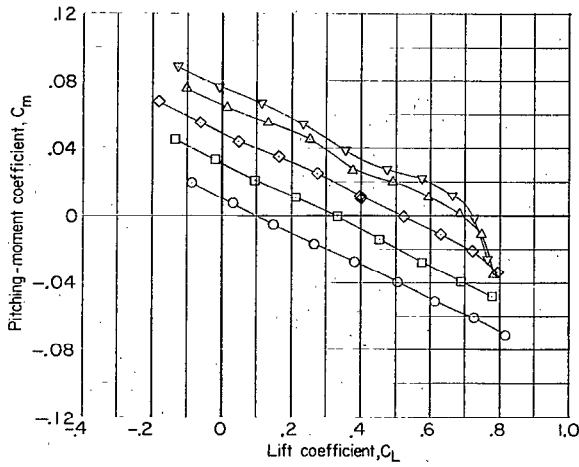
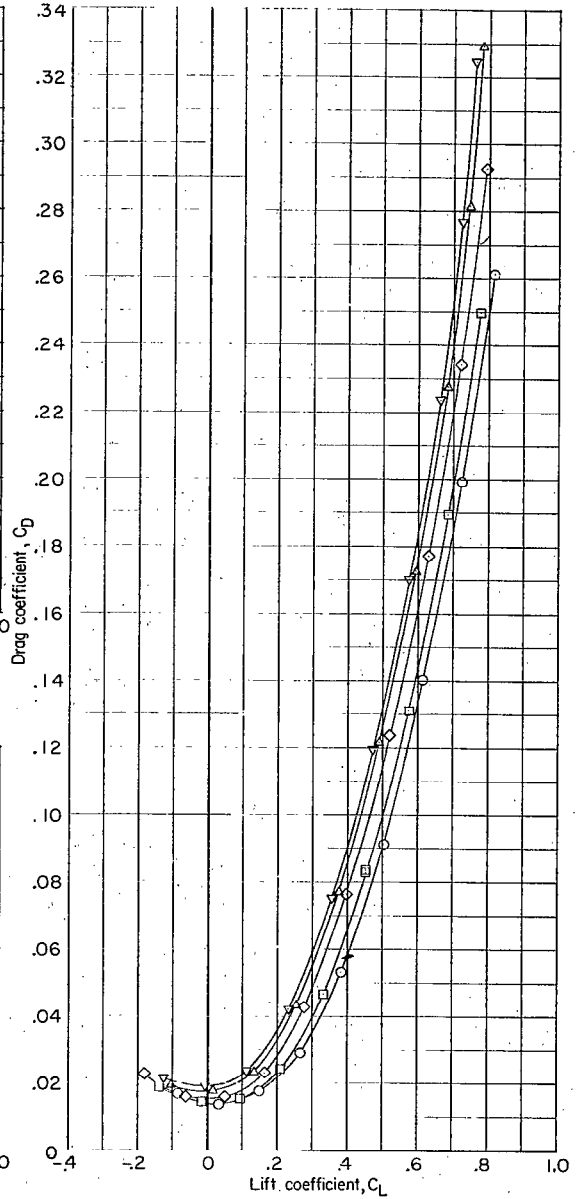
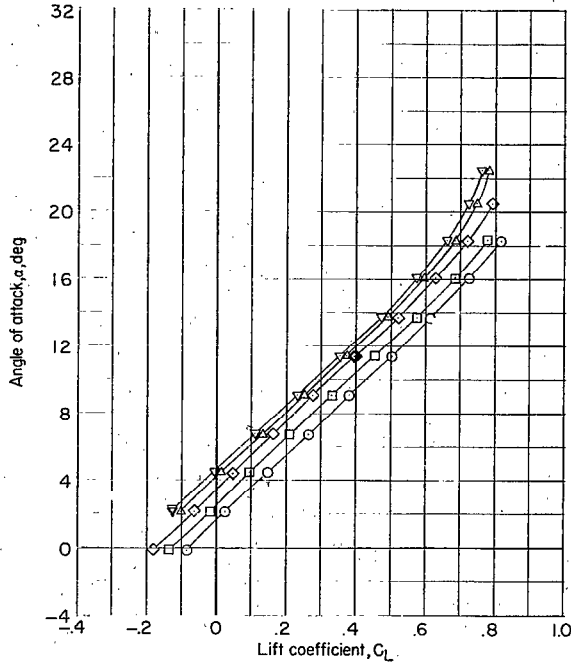
$\delta$ , deg  
 ○ 0  
 □ -2.5  
 ◇ -5.0  
 △ -7.5  
 ▽ -10.0



(b)  $M = 0.85$ .

Figure 4.- Continued.

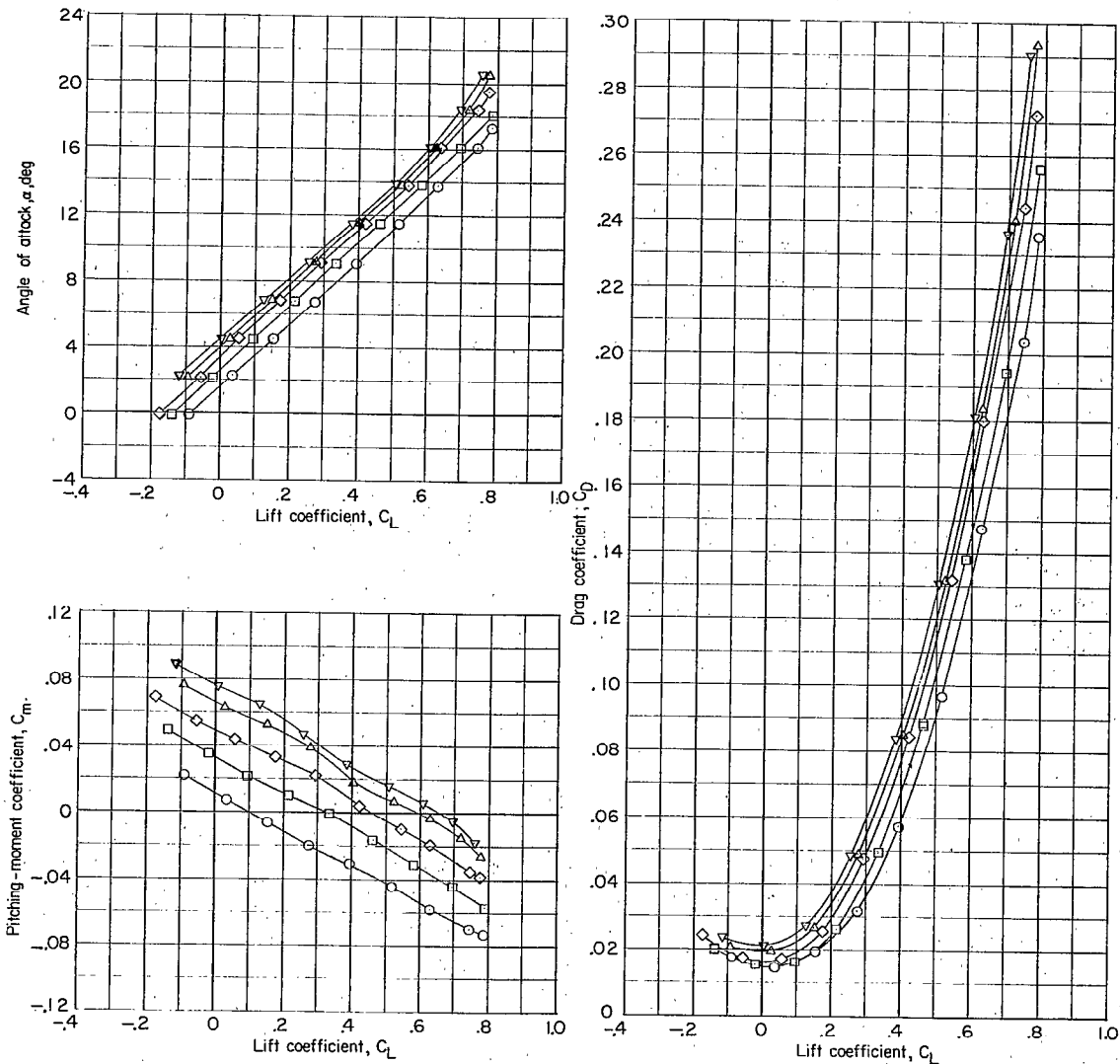
$\delta$ , deg  
○ 0  
□ -2.5  
◇ -5.0  
△ -7.5  
▽ -10.0



(c)  $M = 0.90$ .

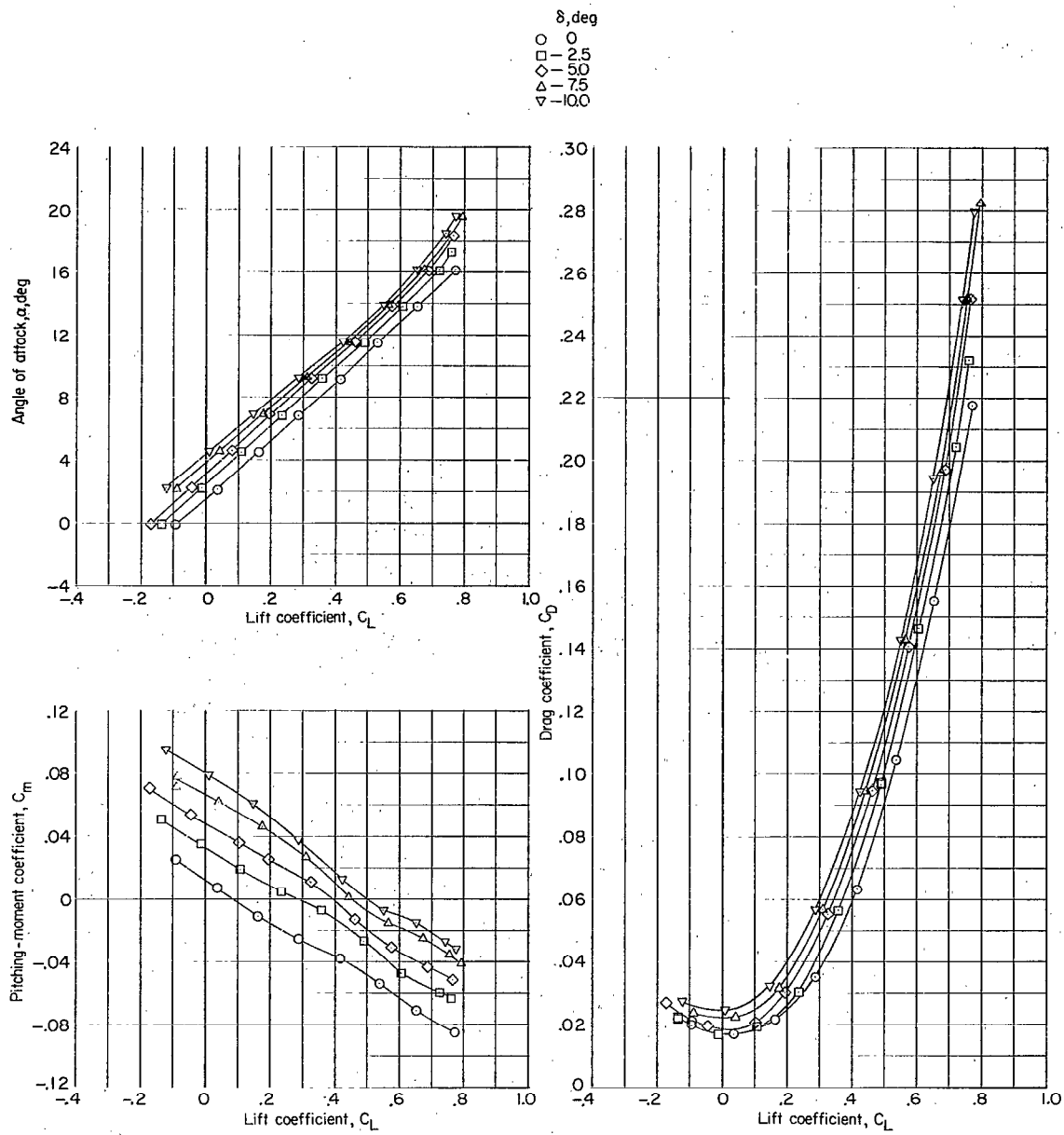
Figure 4.- Continued.

$\delta$ , deg  
○ 0  
□ 1  
◇ 1.5  
△ 1.75  
▽ 10.0



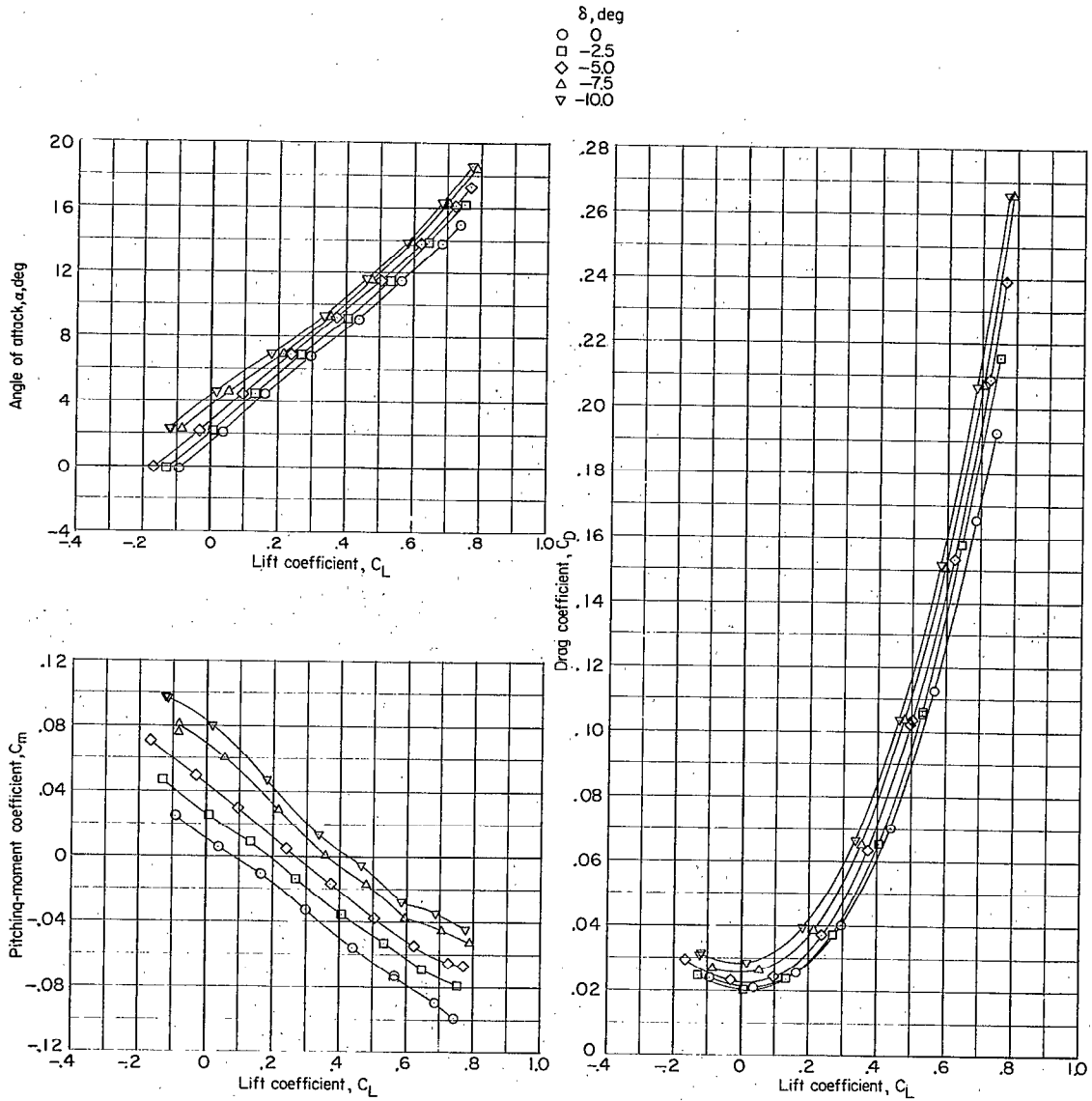
(d)  $M = 0.925$ .

Figure 4.- Continued.



(e)  $M = 0.95$ .

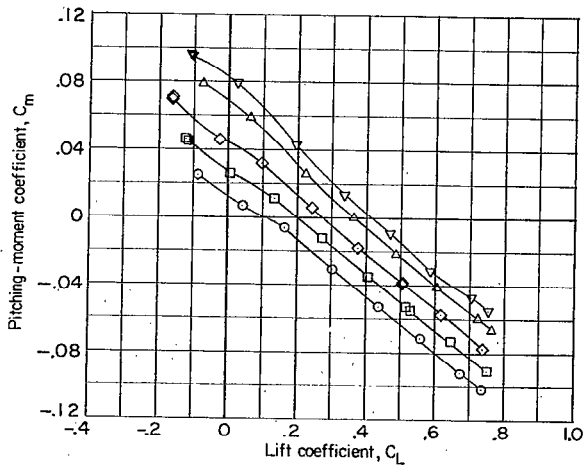
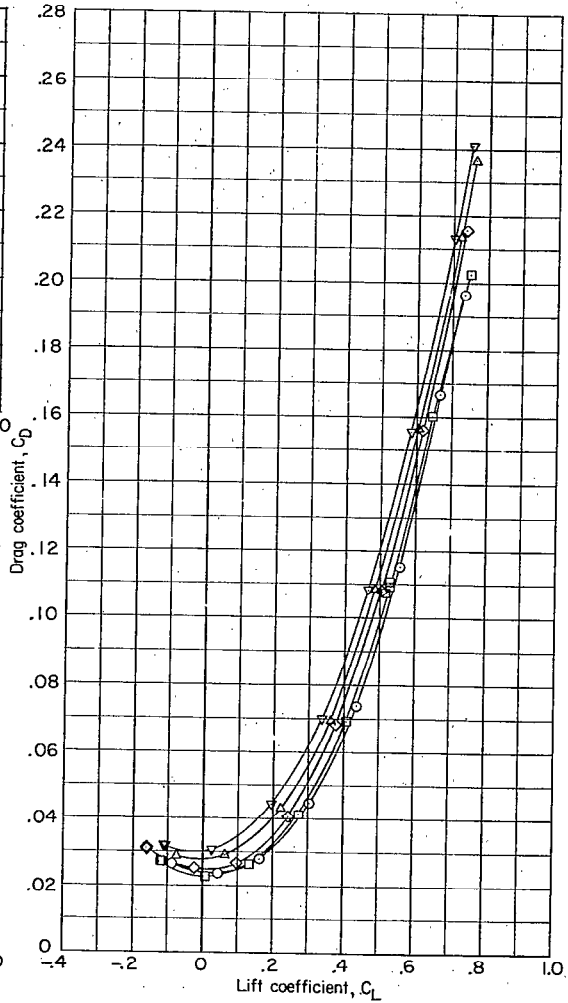
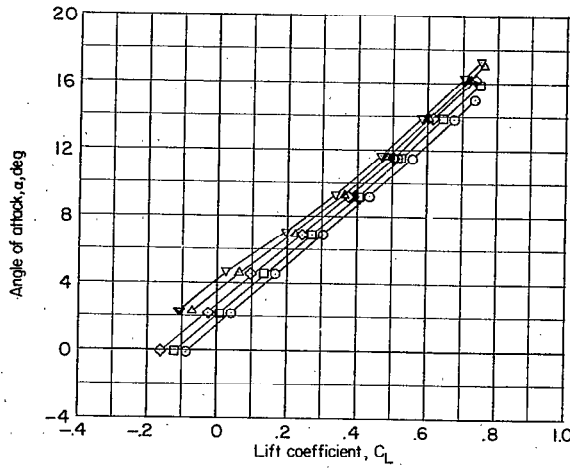
Figure 4.- Continued.



(f)  $M = 0.975$ .

Figure 4.- Continued.

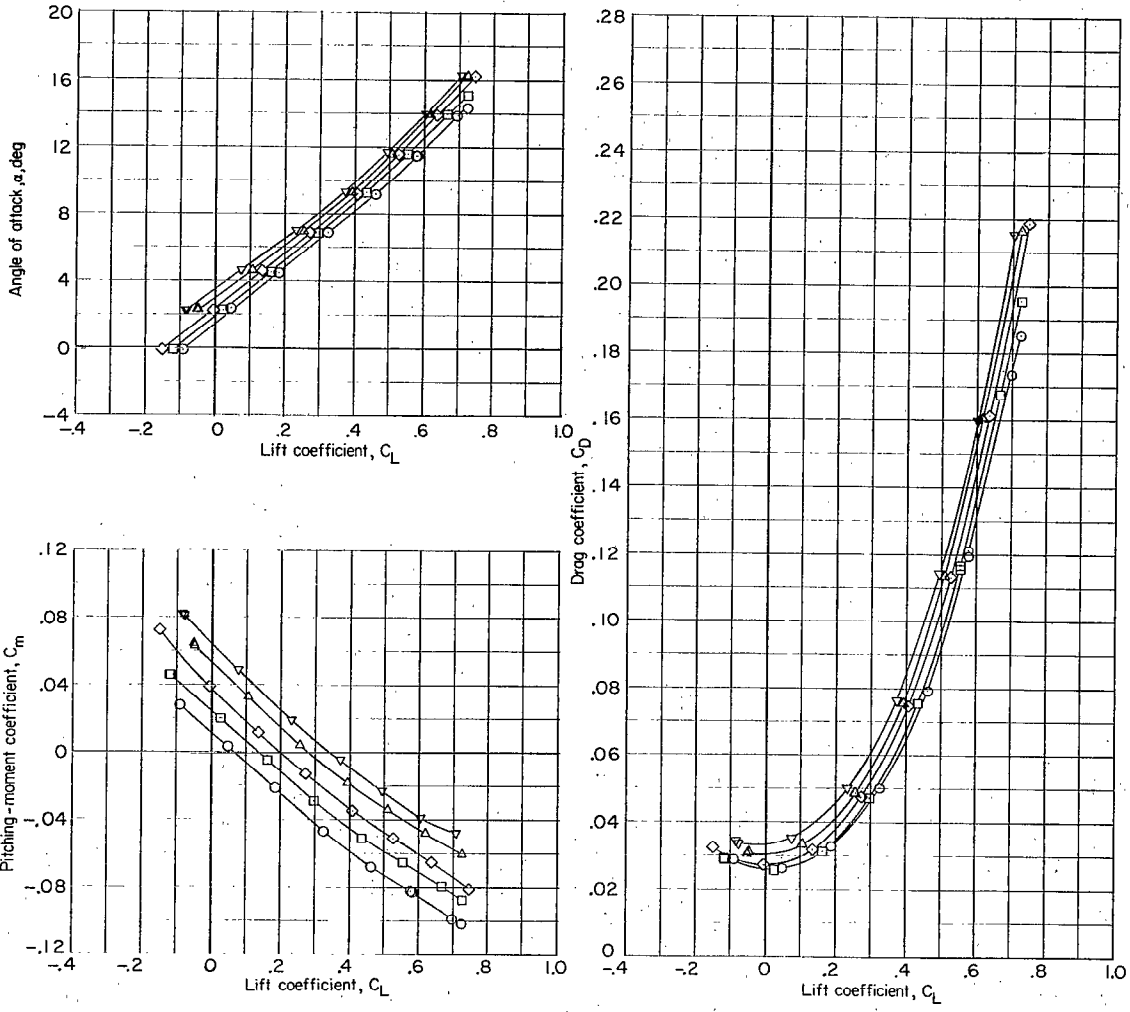
$\delta$ , deg  
 ○ 0  
 □ -2.5  
 ◇ -5.0  
 △ -7.5  
 ▽ -10.0



(g)  $M = 1.00$ .

Figure 4.- Continued.

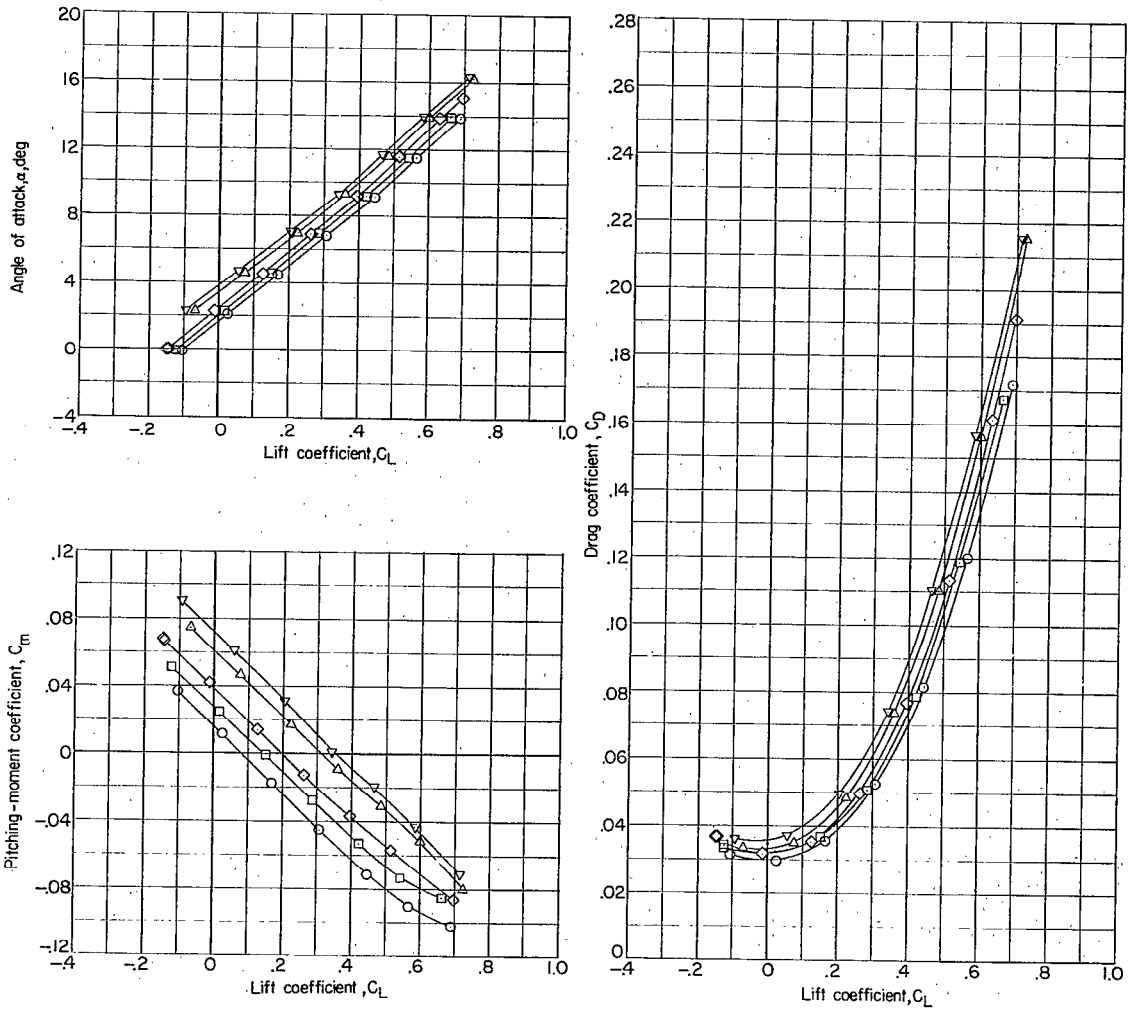
$\delta$ , deg  
○ 0  
□ -2.5  
◇ -5.0  
△ -7.5  
▽ -10.0



(h)  $M = 1.025$ .

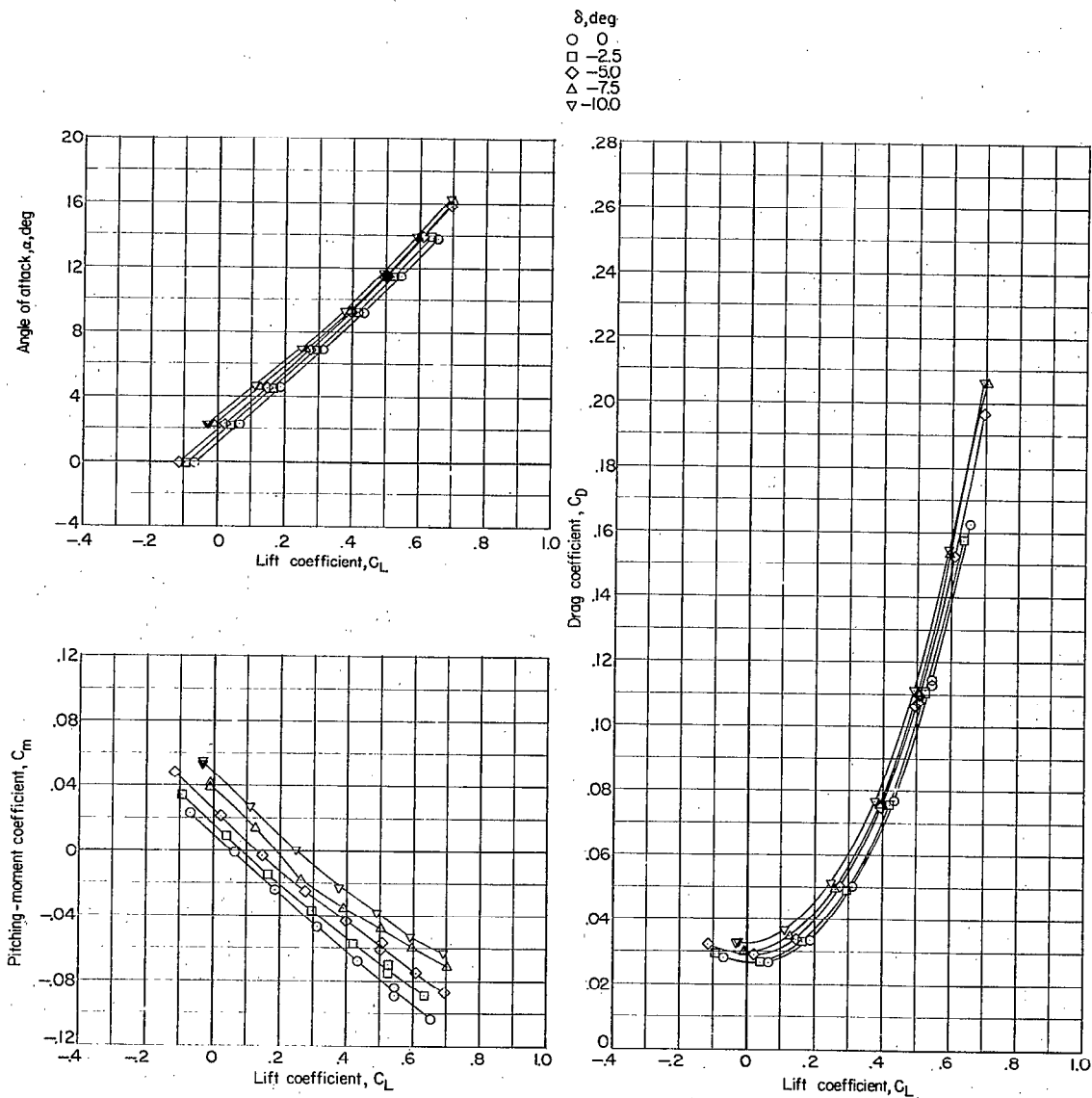
Figure 4.- Continued.

$\delta$ , deg  
 ○ 0  
 □ -2.5  
 ◇ -5.0  
 △ -7.5  
 ▽ -10.0



(i)  $M = 1.075$ .

Figure 4.- Continued.



(j)  $M = 1.135$ .

Figure 4.- Concluded.

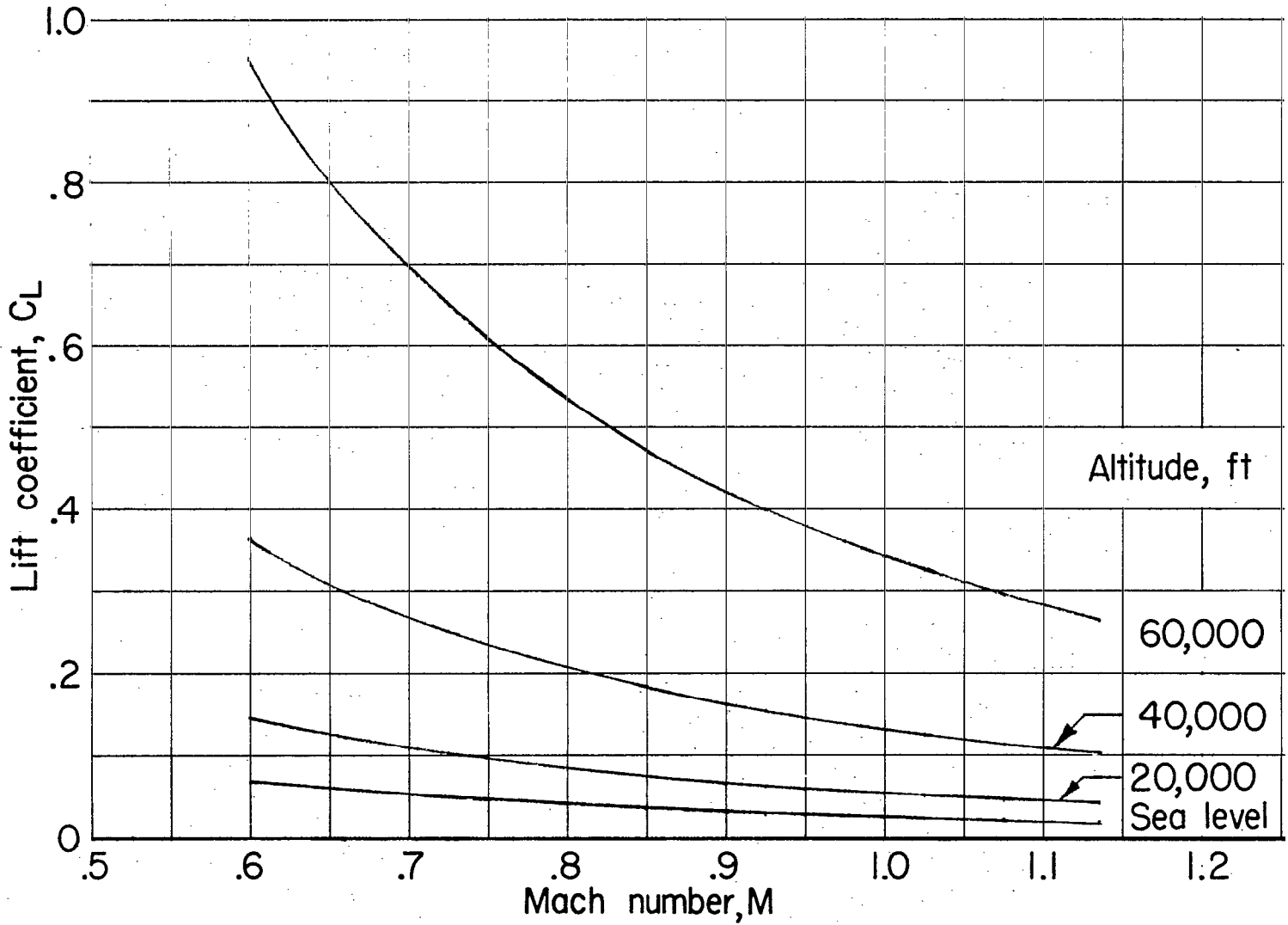


Figure 5.- Variation with Mach number of the lift coefficient required for level flight at several altitudes for a wing loading of 36 lb/sq ft.

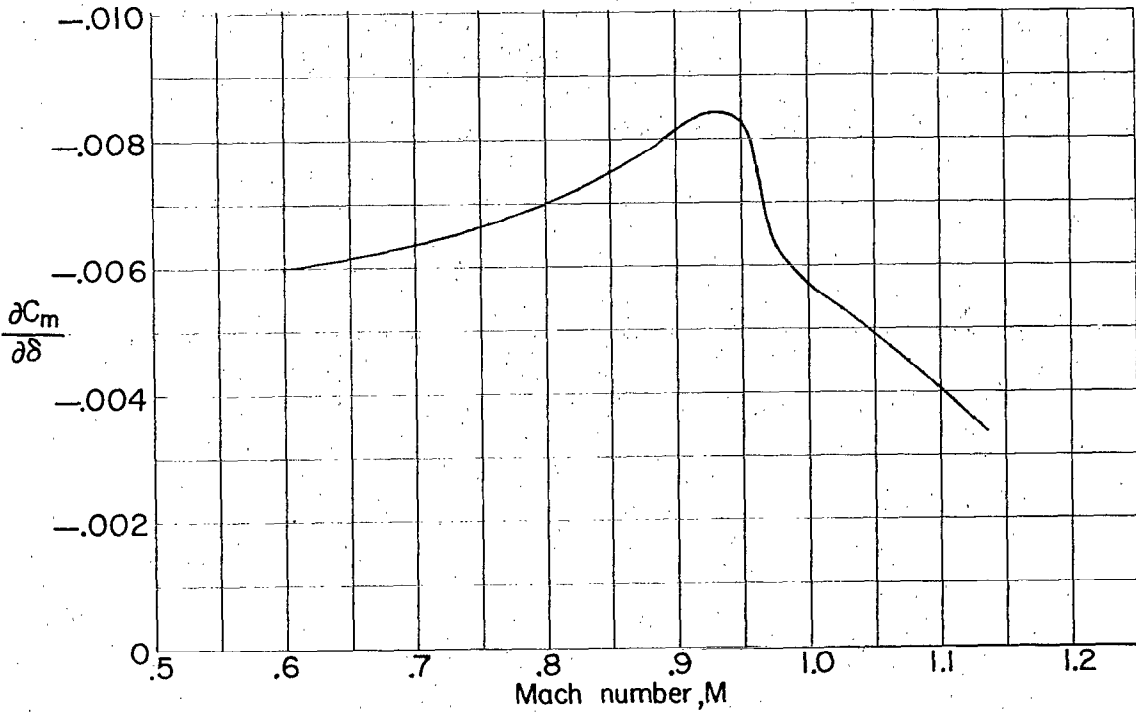
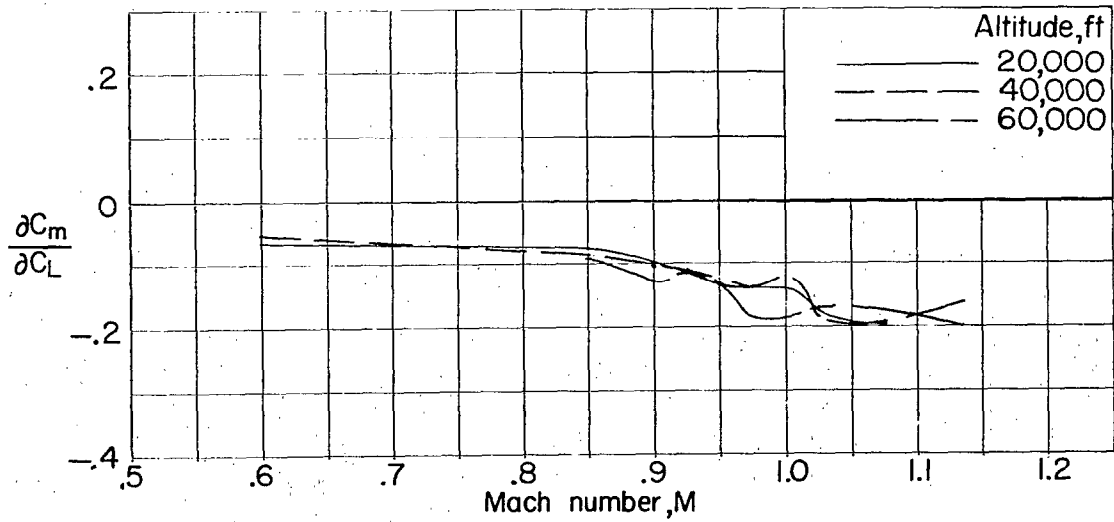


Figure 6.- Variation with Mach number of the trimmed static longitudinal stability parameter and the elevator pitch effectiveness parameter.

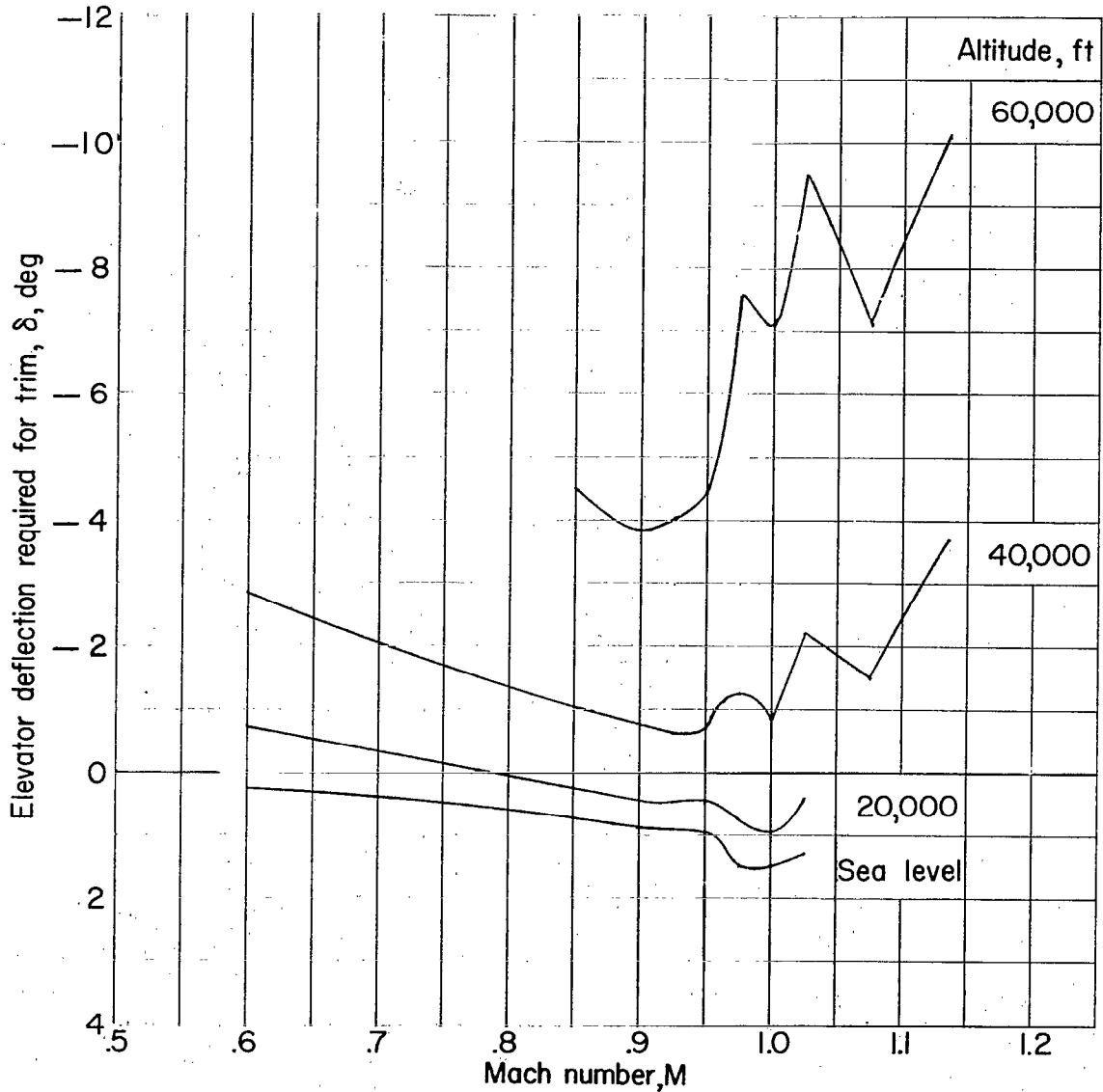


Figure 7.- Variation with Mach number of elevator deflection required for trimmed level flight at several altitudes for a wing loading of 36 lb/sq ft.

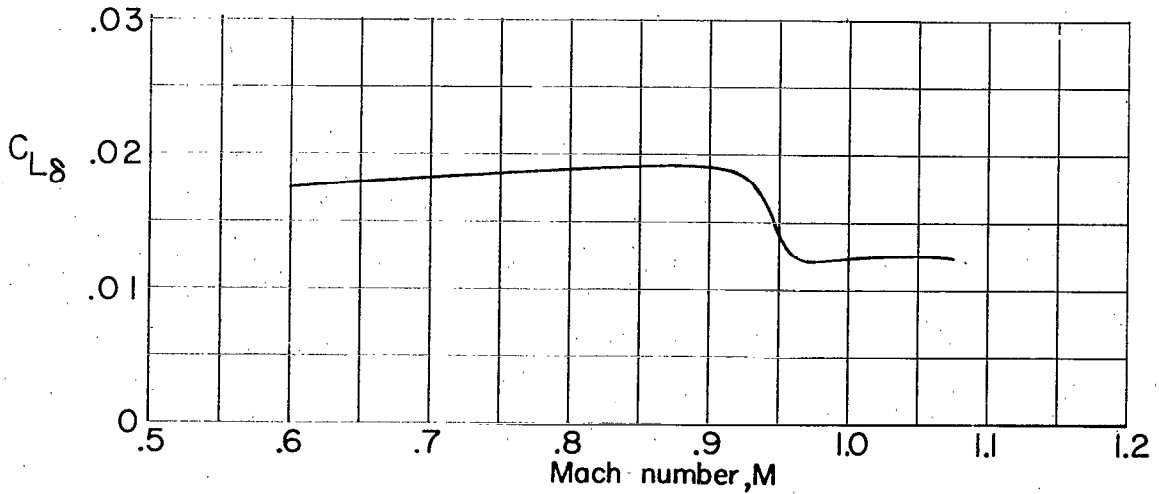
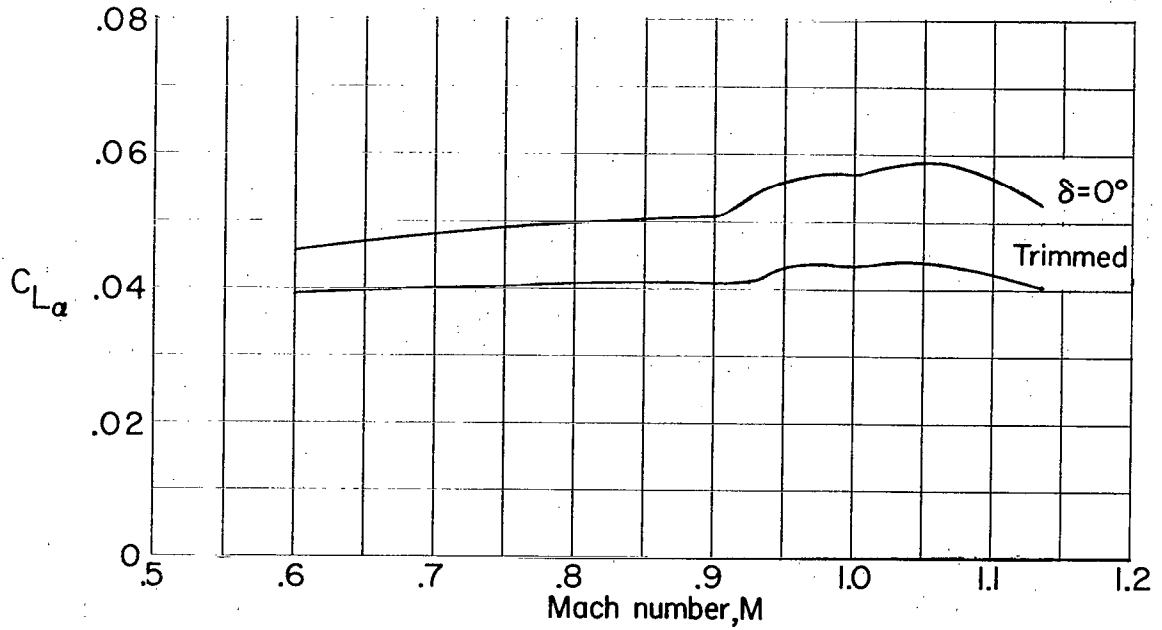


Figure 8.- Variation with Mach number of the lift-curve slope and the elevator lift effectiveness parameter.

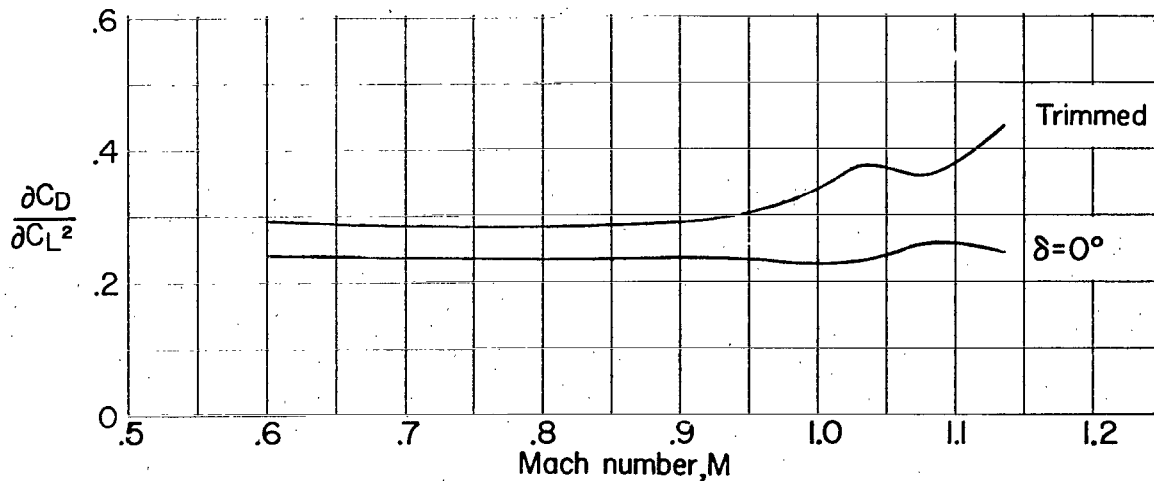
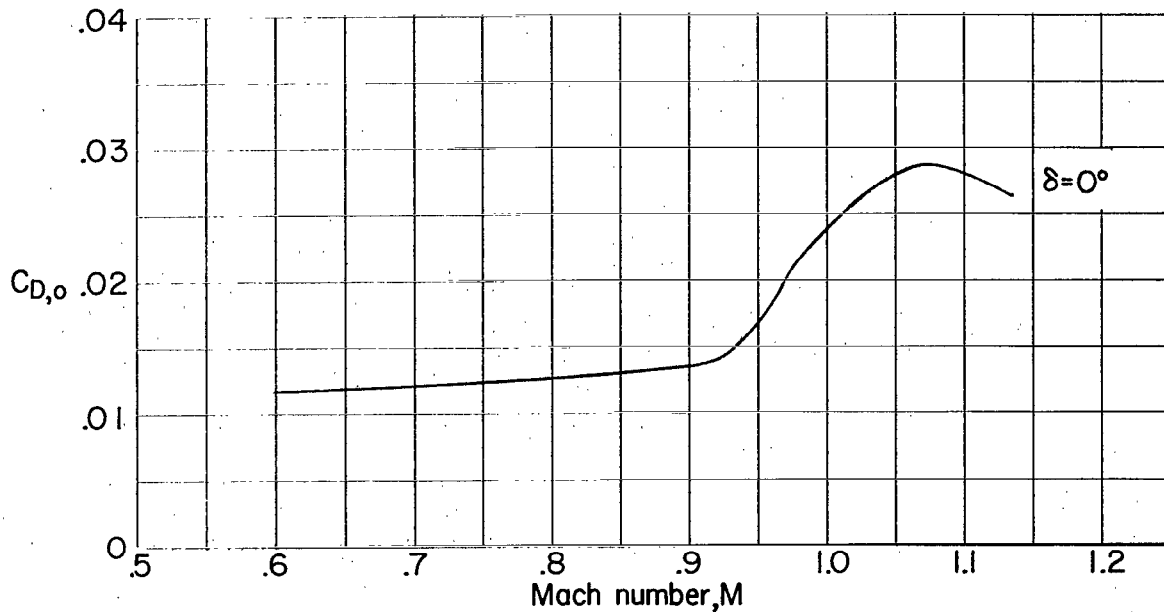


Figure 9.- Variation with Mach number of the drag coefficient at zero lift and the drag-due-to-lift factor, averaged over a lift-coefficient range from 0 to 0.3.

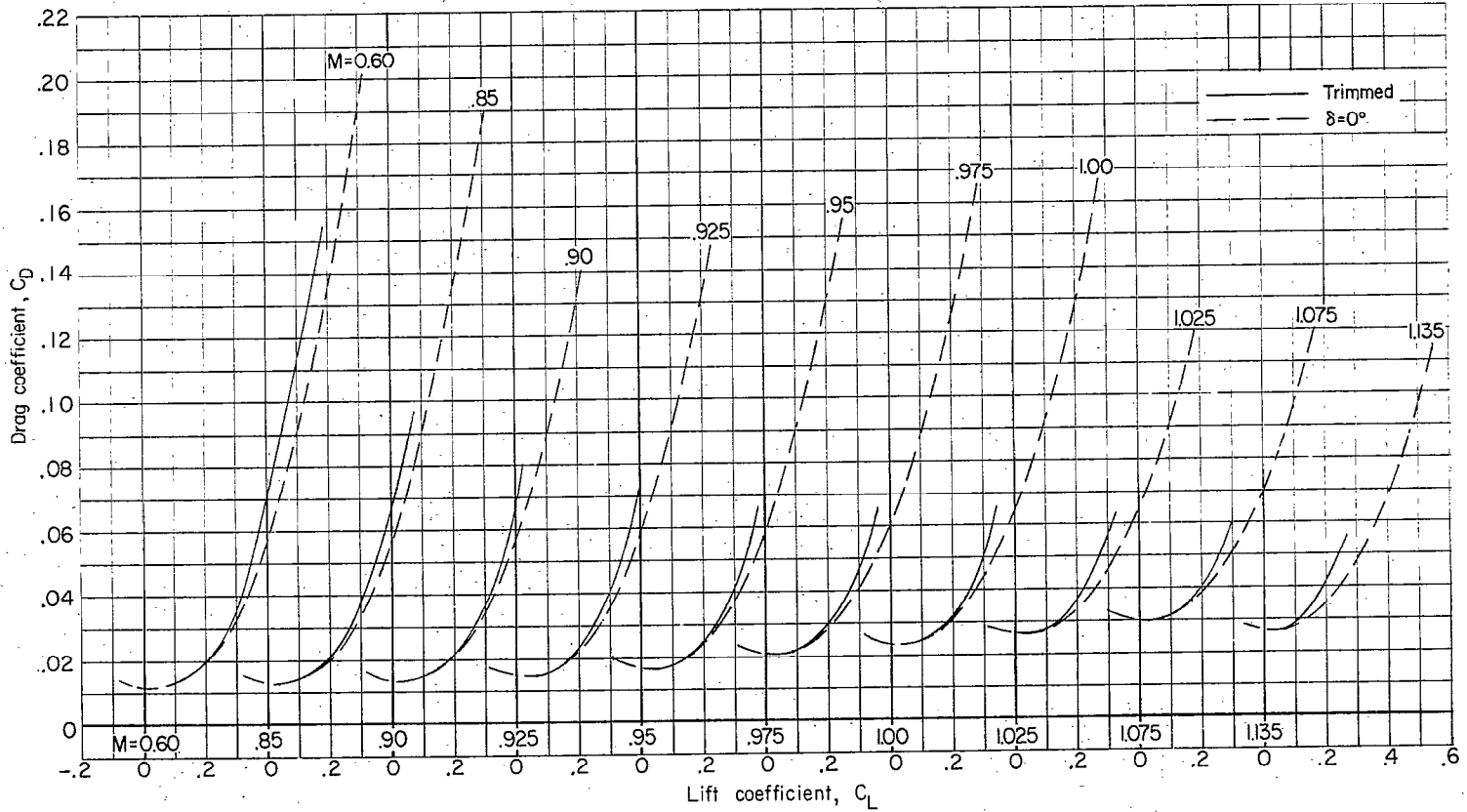


Figure 10.- Variation of drag coefficient with lift coefficient.

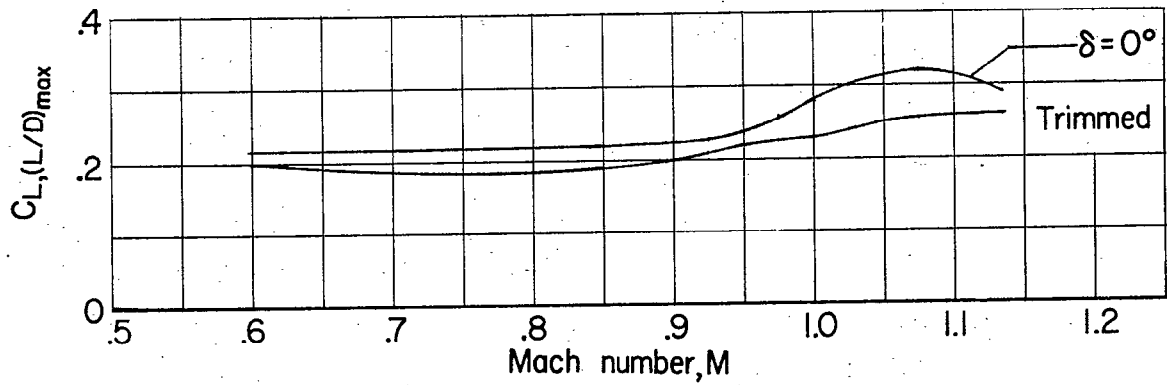
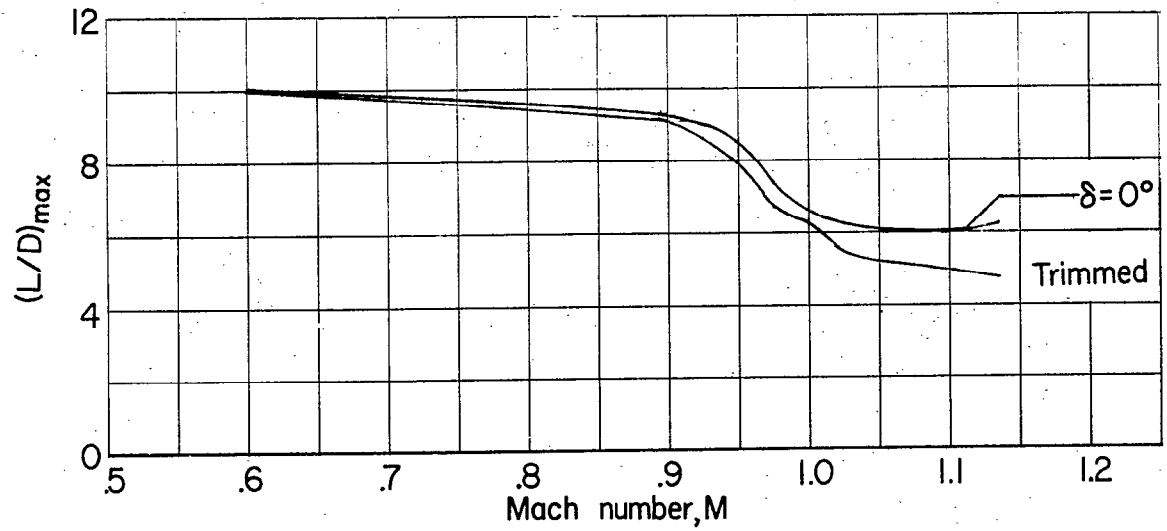
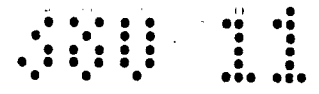


Figure 11.- Variation with Mach number of the maximum lift-drag ratio and lift coefficient for maximum lift-drag ratio.

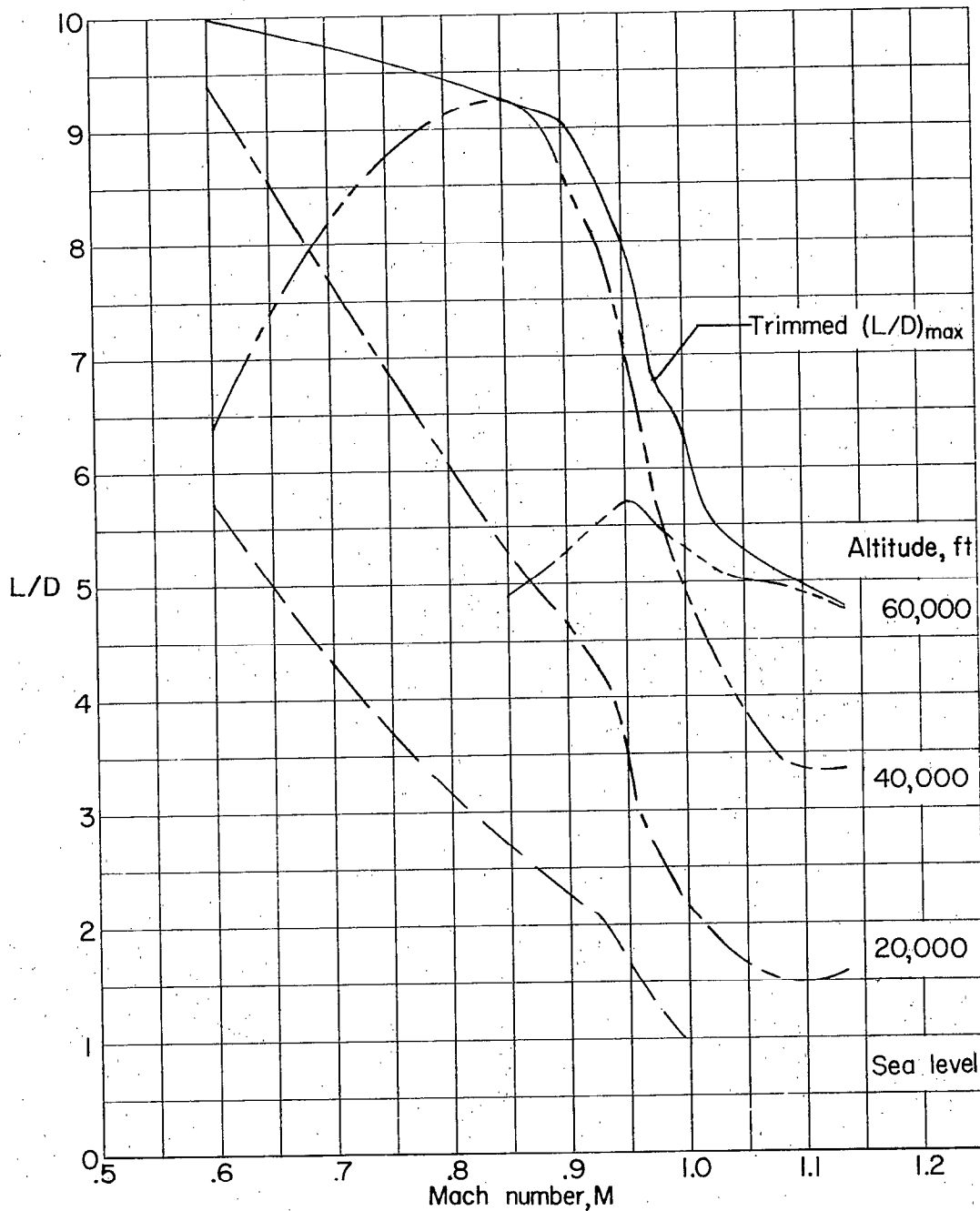


Figure 12.- Variation with Mach number of the maximum trimmed lift-drag ratio and of the trimmed lift-drag ratio in level flight at several altitudes for a wing loading of 36 lb/sq ft.

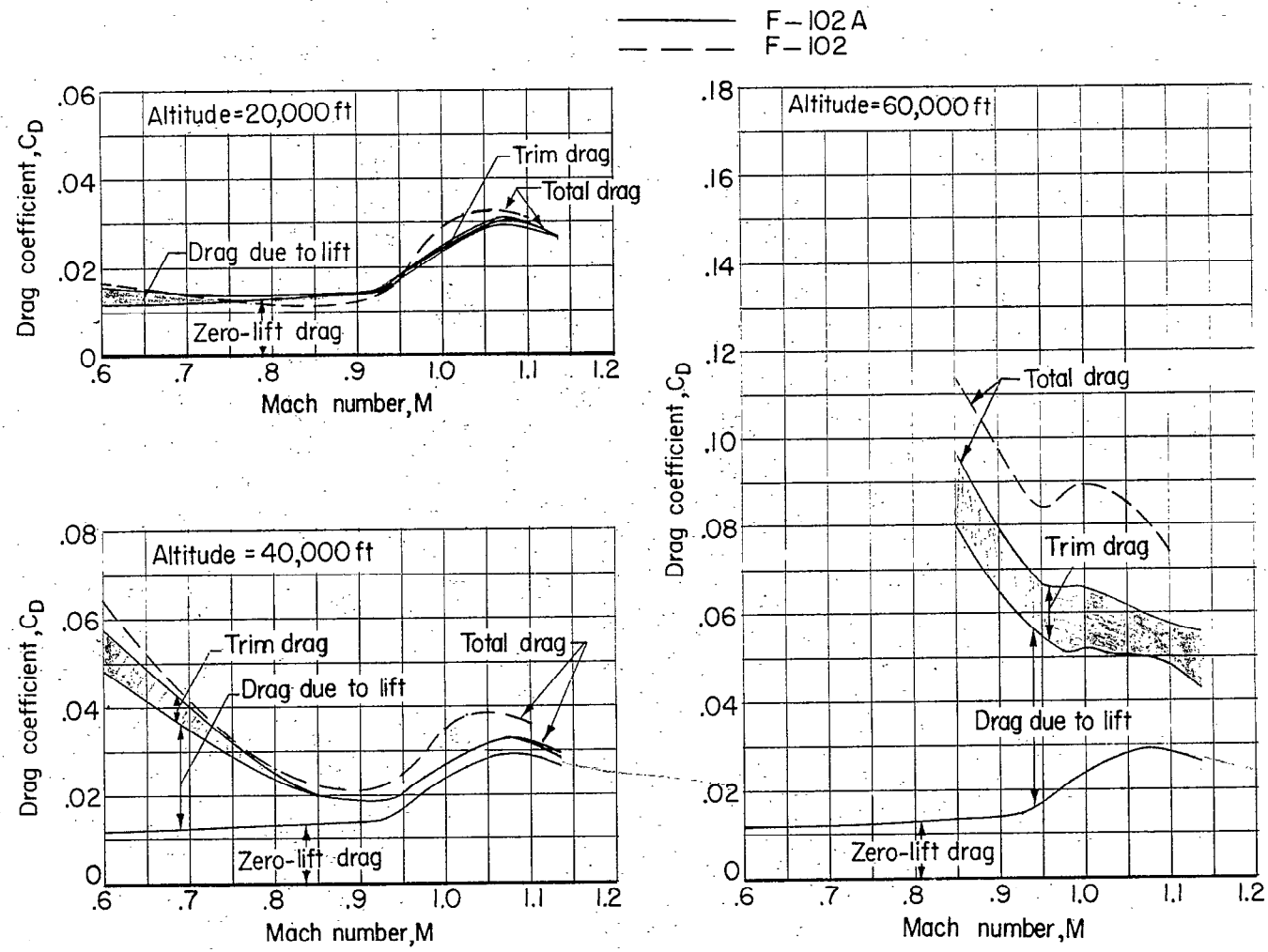
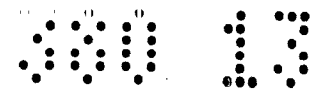


Figure 13.- Variation with Mach number of the total drag coefficient for trimmed level flight at several altitudes for the F-102 and the F-102A airplane configuration with a drag-coefficient breakdown for the F-102A.

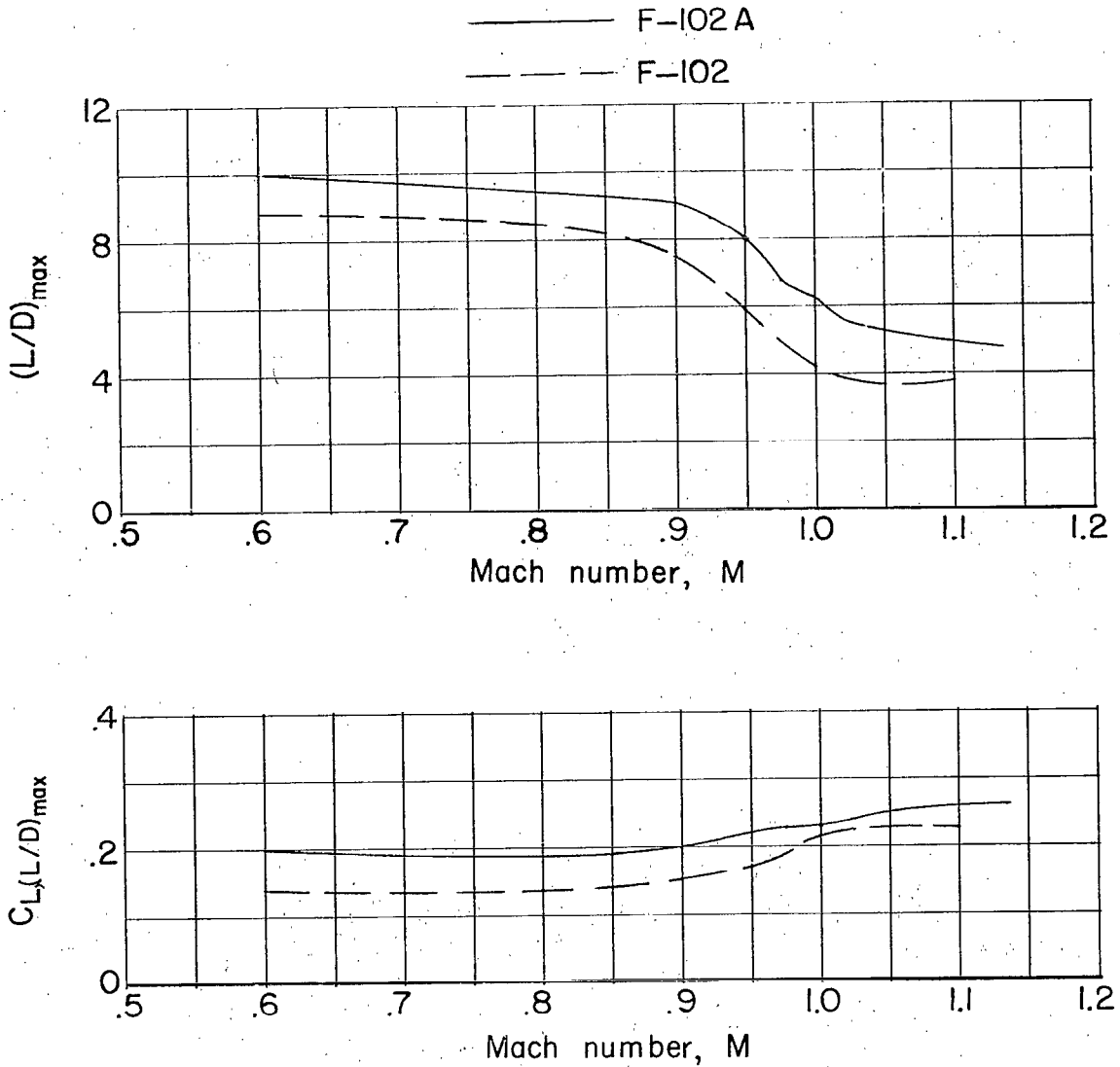
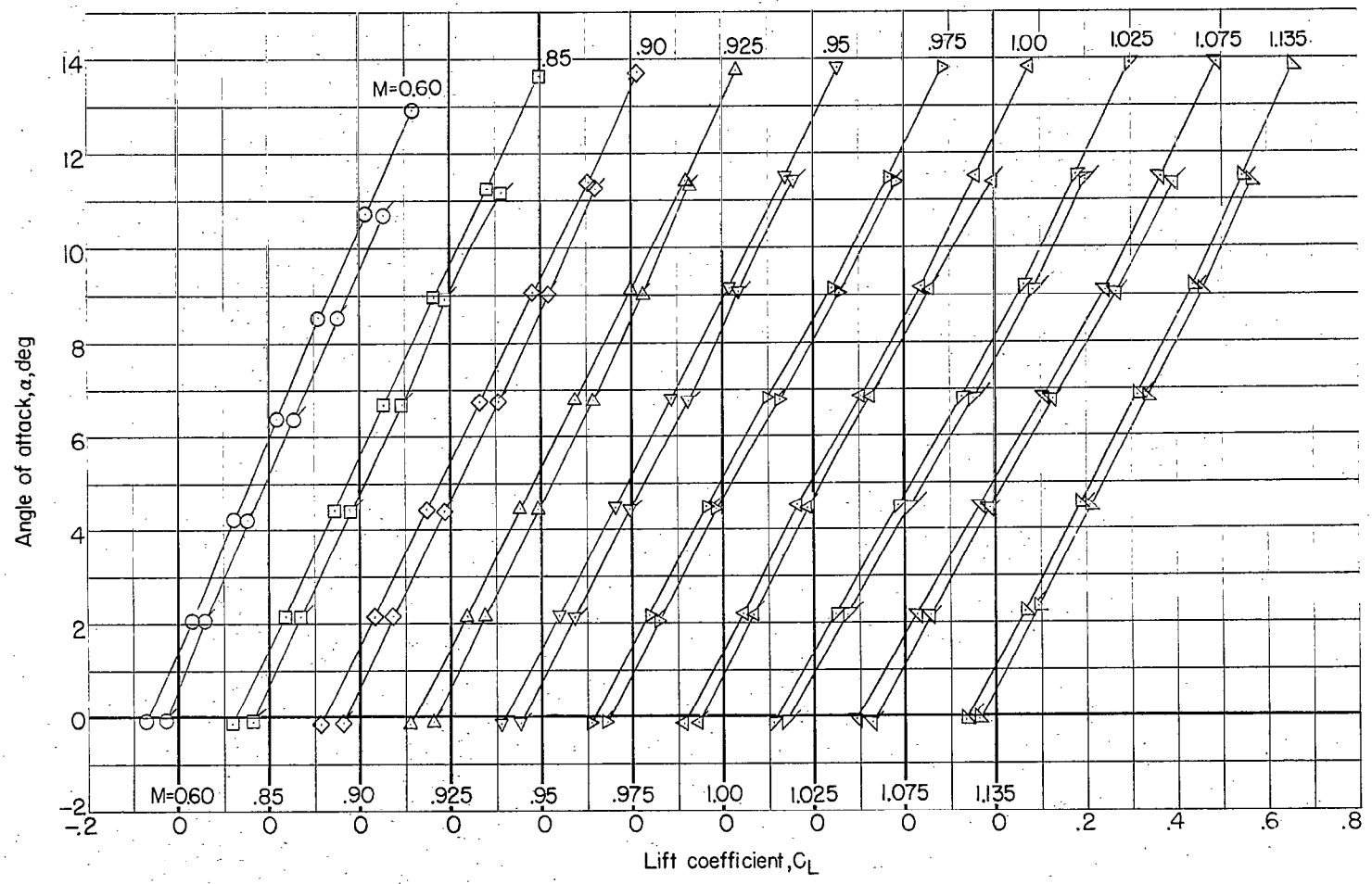
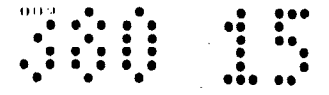
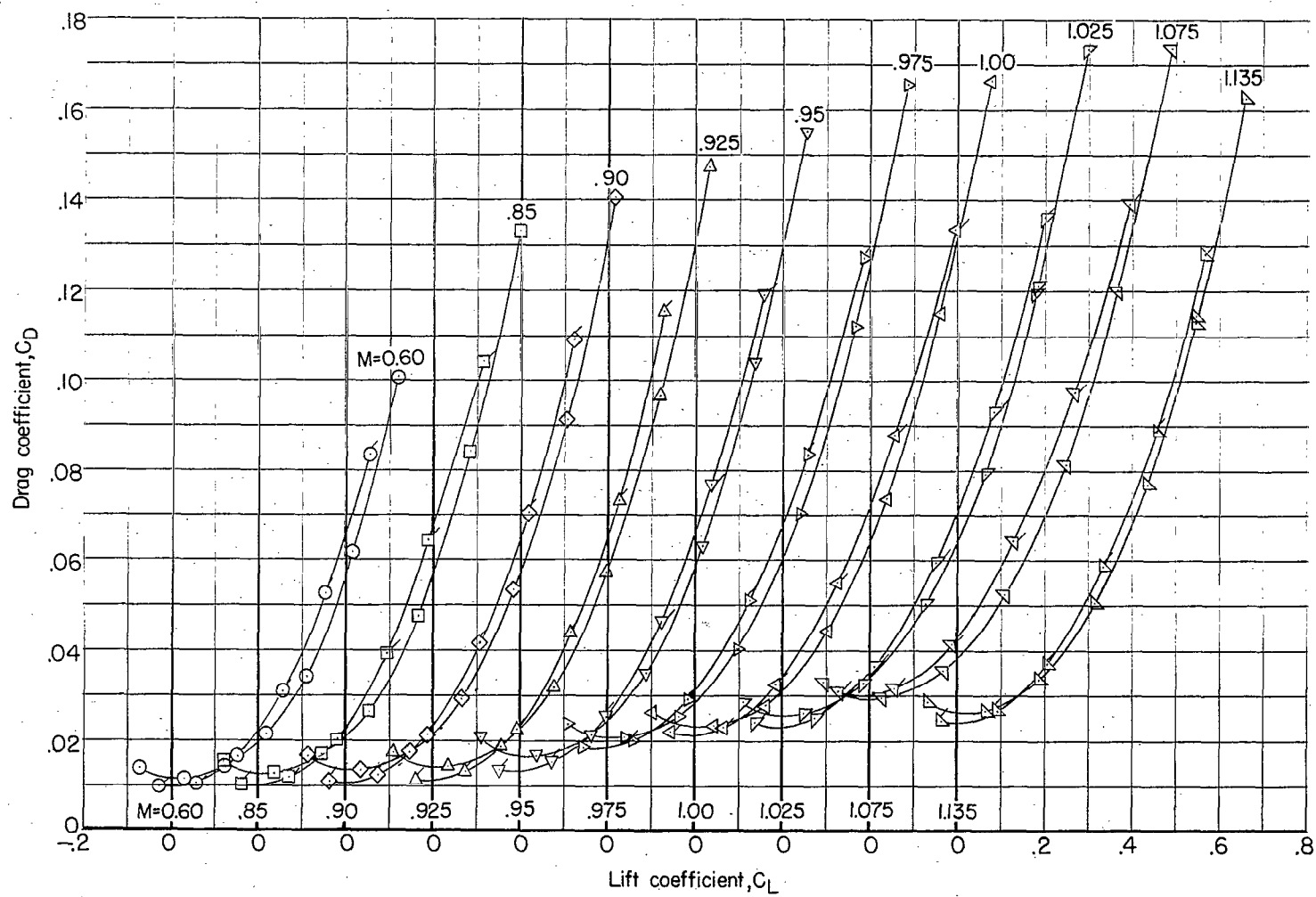
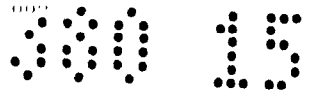


Figure 14.- Variation with Mach number of the maximum trimmed lift-drag ratio and the lift coefficient for maximum trimmed lift-drag ratio for the F-102 and the F-102A airplane configurations.



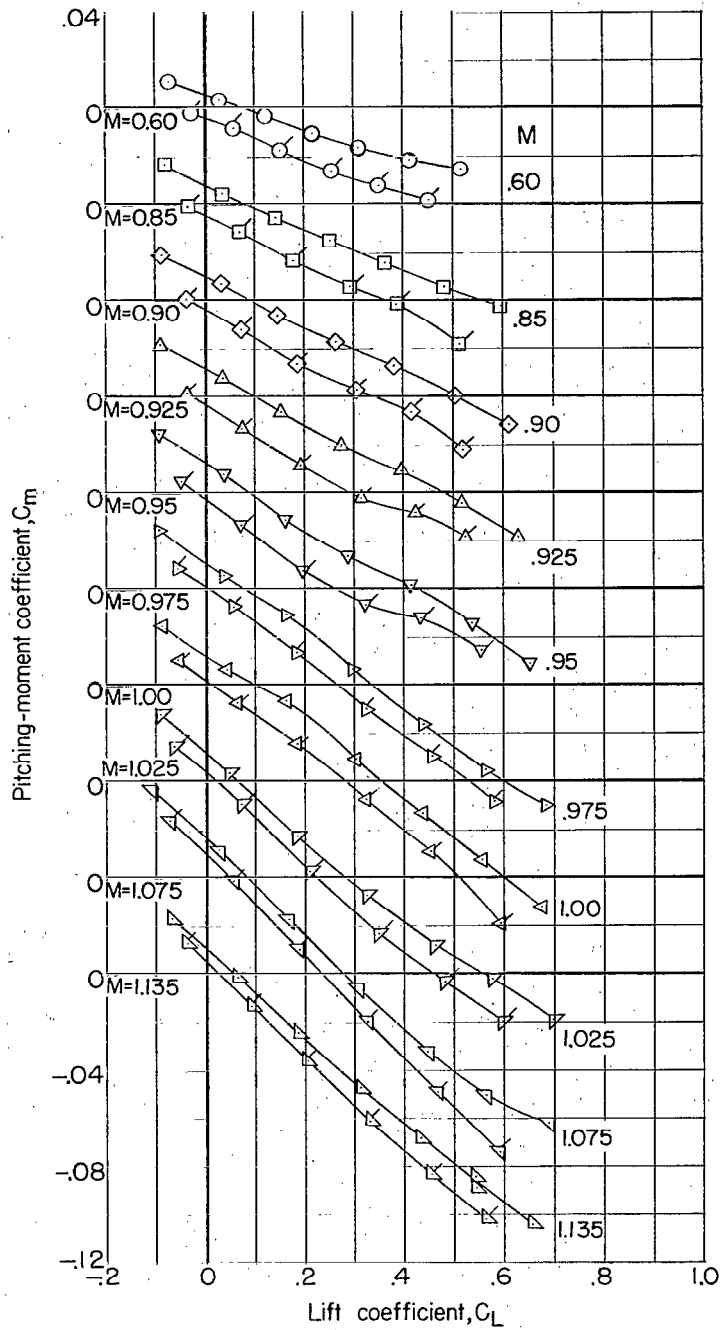
(a) Variation of angle of attack with lift coefficient.

Figure 15.- Longitudinal characteristics of the basic F-102A model configuration (with leading-edge camber and deflected tips) and the plane-wing model configuration.  $\beta = 0^\circ$ . (Plain symbols indicate data for the basic wing; flagged symbols indicate data for the plane wing.)



(b) Variation of drag coefficient with lift coefficient.

Figure 15.- Continued.



(c) Variation of pitching-moment coefficient with lift coefficient.

Figure 15.- Concluded.

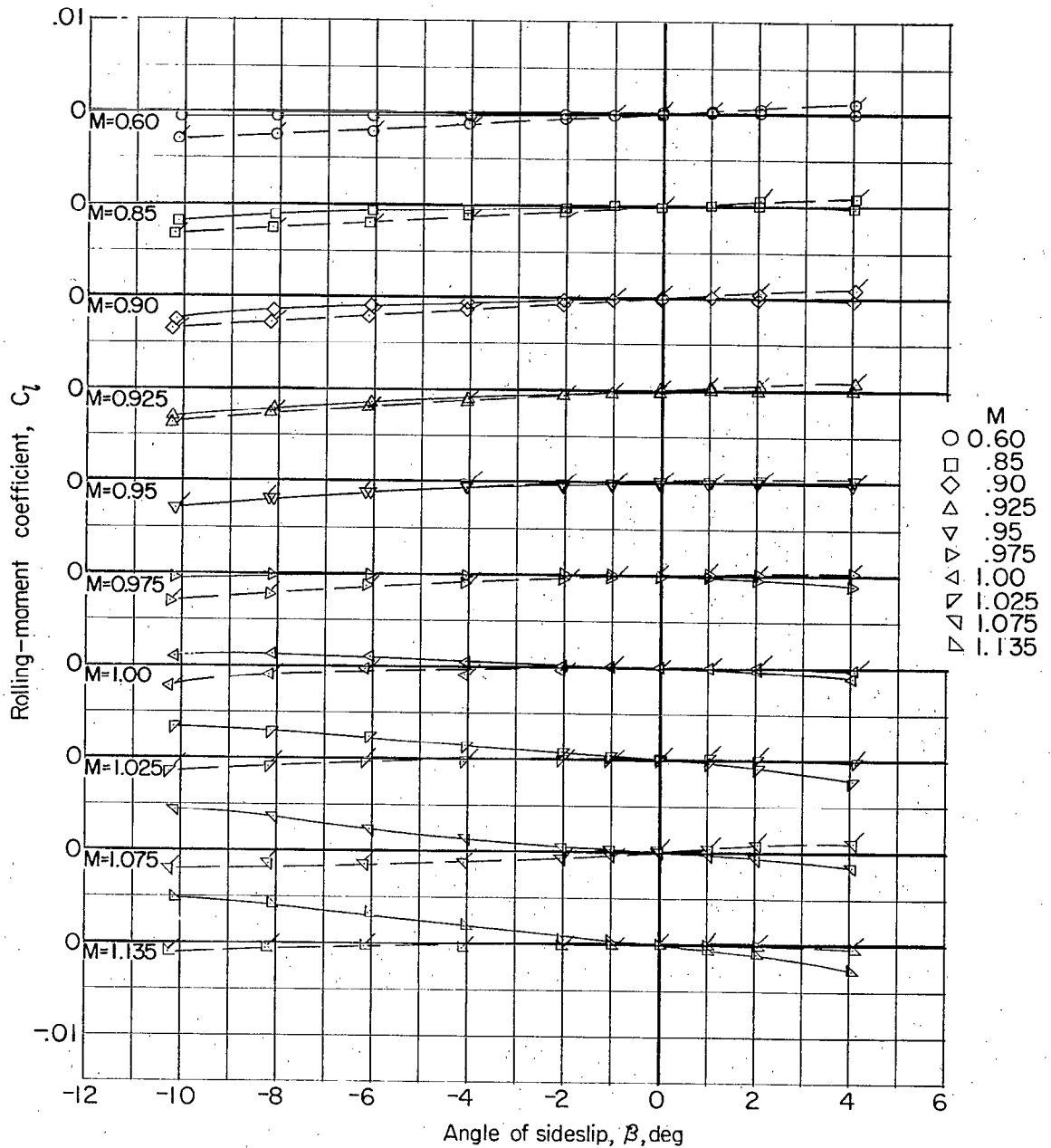


Figure 16.- Variation of rolling-moment coefficient with angle of sideslip at constant Mach number.  $\alpha = 2.2^\circ$ . (Plain symbols indicate configuration with tail data; flagged symbols, without tail data.)

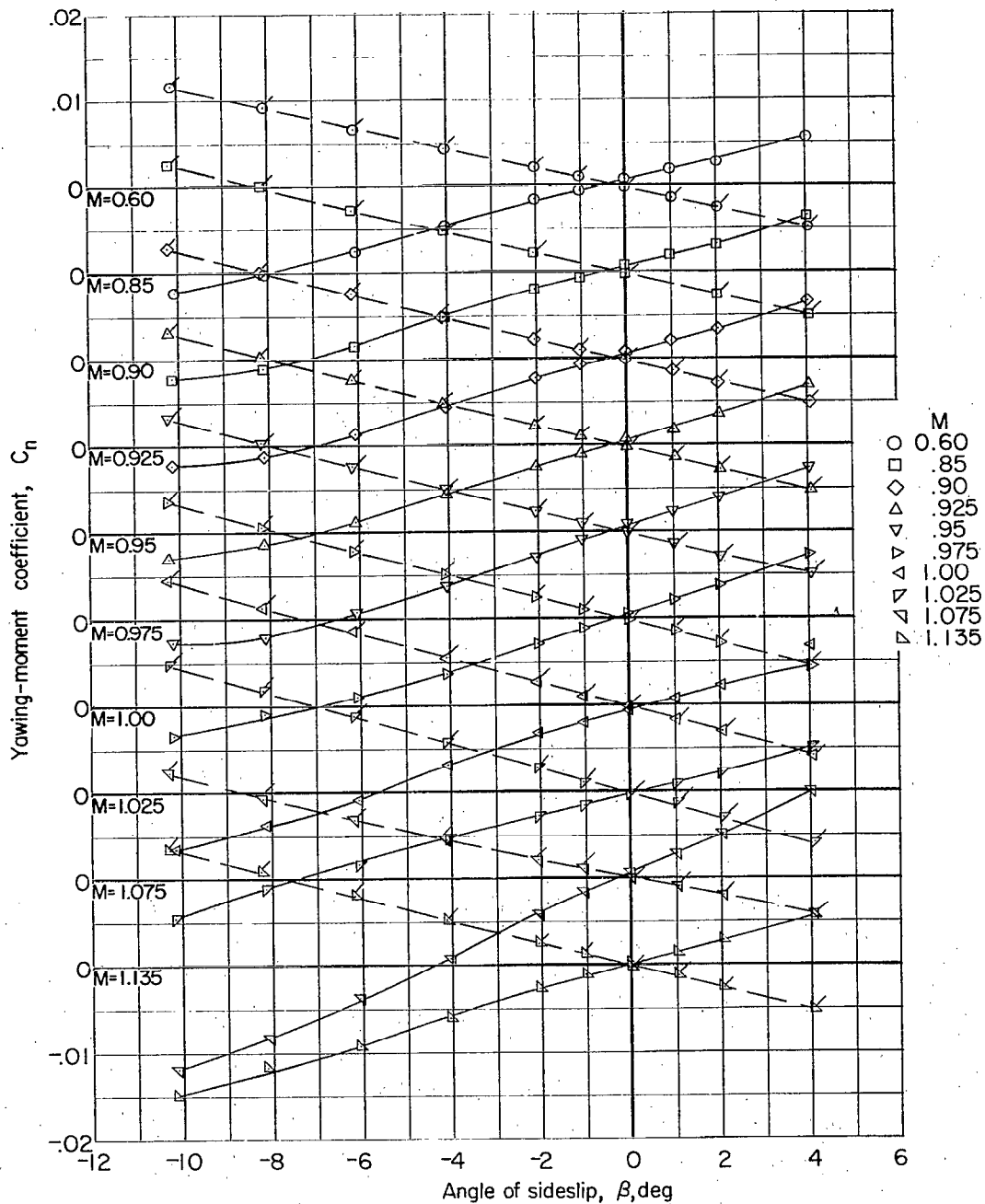


Figure 17.- Variation of yawing-moment coefficient with angle of sideslip at constant Mach number.  $\alpha = 2.2^\circ$ . (Plain symbols indicate configuration with tail data; flagged symbols, without tail data.)

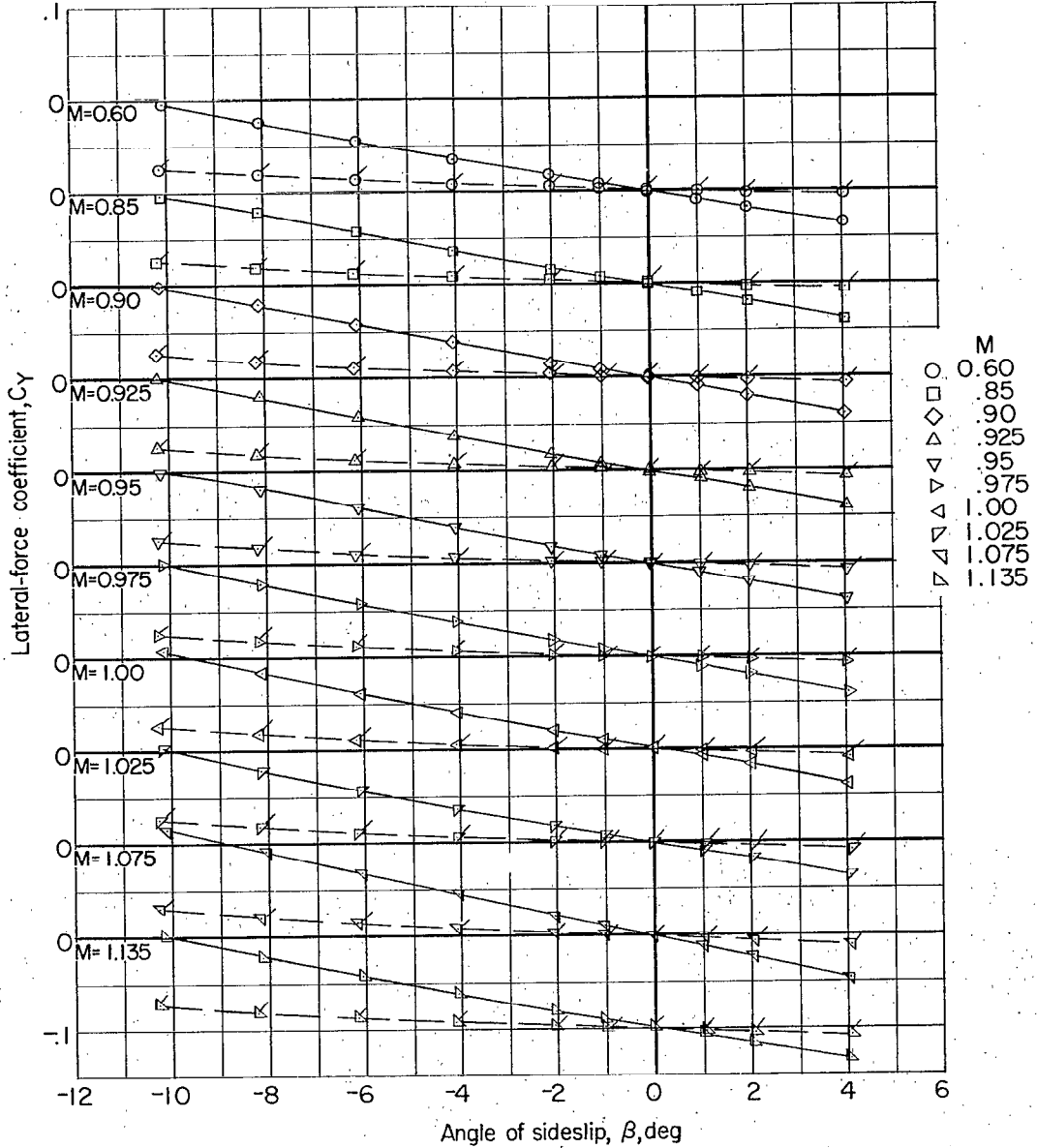


Figure 18.- Variation of lateral-force coefficient with angle of sideslip at constant Mach number.  $\alpha = 2.2^\circ$ . (Plain symbols indicate configuration with tail data; flagged symbols, without tail data.)

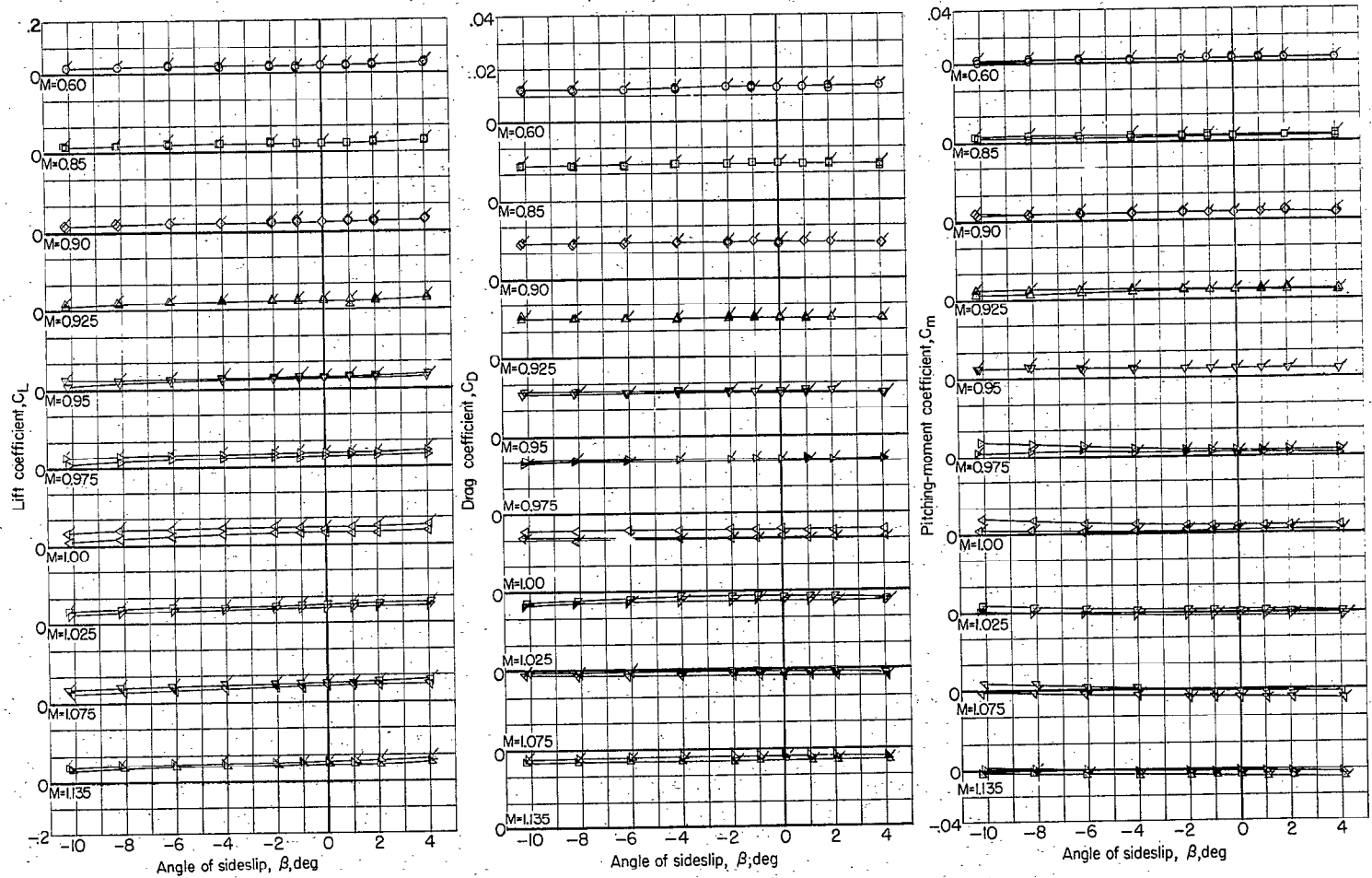


Figure 19.- Variation of basic model lift, drag, and pitching-moment coefficients with angle of sideslip at a constant angle of attack of  $2.2^\circ$ .  $\delta = 0^\circ$ . (Plain symbols indicate configuration with tail data; flagged symbols, without tail data.)

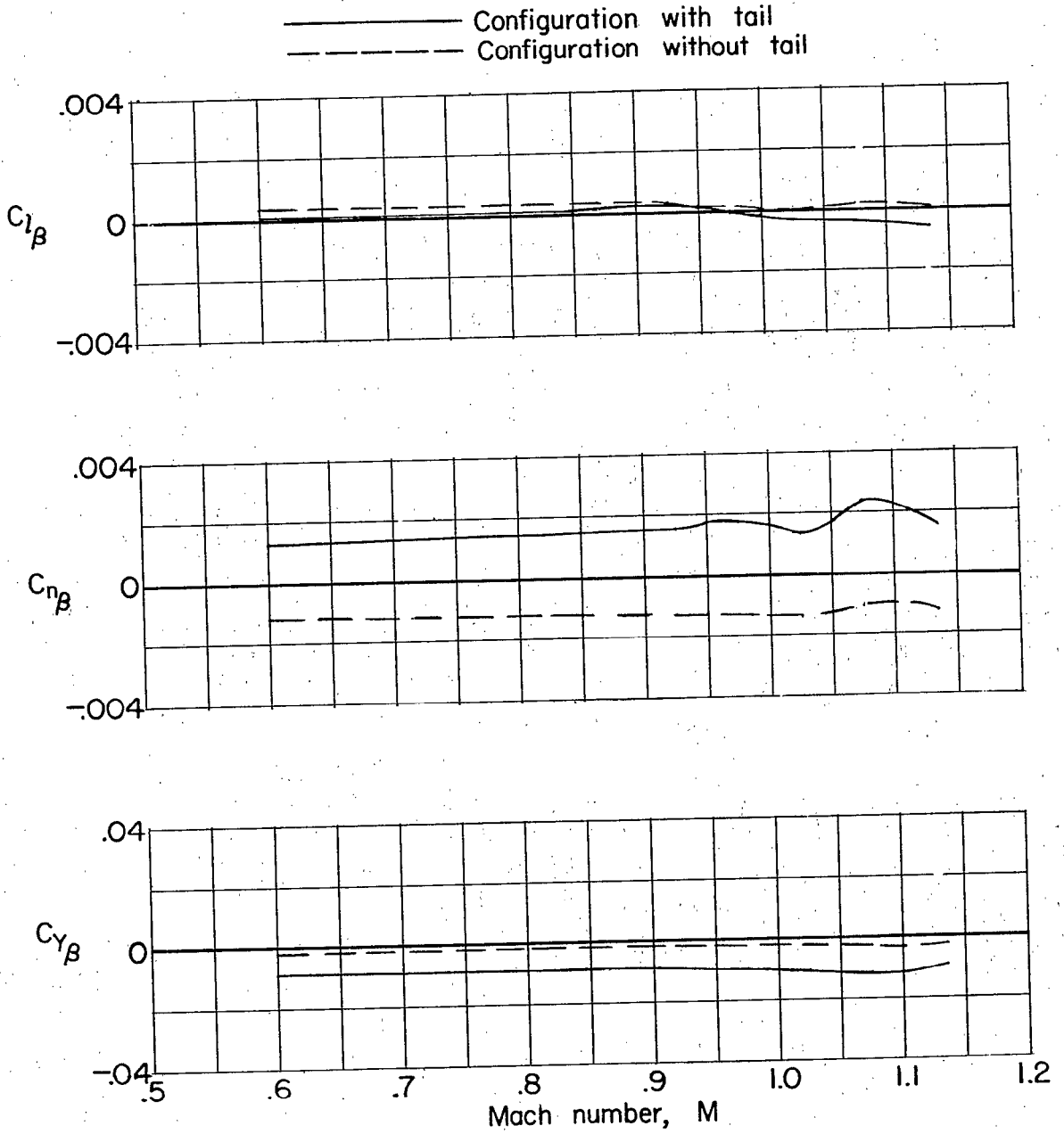


Figure 20.- Lateral-directional characteristics of the basic model at a constant angle of attack of  $2.2^\circ$ .  $\delta = 0^\circ$ .

STATIC STABILITY AND CONTROL CHARACTERISTICS OF A  
0.04956-SCALE MODEL OF THE CONVAIR F-102A  
AIRPLANE AT TRANSONIC SPEEDS

By Walter B. Olstad and Robert S. Osborne

ABSTRACT

The effects of elevator deflections from  $0^\circ$  to  $-10^\circ$  on the force and moment characteristics of a 0.04956-scale model of the Convair F-102A airplane have been determined at Mach numbers from 0.60 to 1.135 for angles of attack up to  $20^\circ$  in the Langley 8-foot transonic tunnel. The model was also tested with a plane wing to indicate the effects of wing leading-edge camber and deflected tips. In addition, the basic model was tested at angles of sideslip from  $-10^\circ$  to  $4^\circ$  at an angle of attack of  $2.2^\circ$ .

INDEX HEADINGS

Wing-Fuselage Combinations - Airplanes	1.7.1.1.1
Airplanes - Specific Types	1.7.1.2
Stability, Longitudinal - Static	1.8.1.1.1
Stability, Directional - Static	1.8.1.1.3
Control, Longitudinal	1.8.2.1